

The Investigation of Mysterious Marine Oil Spills on the West Coast of Canada

by

Andrew Szeto

Submitted in partial fulfilment of the requirements
for the degree of Master of Applied Science

at

Dalhousie University
Halifax, Nova Scotia
August 2012

© Copyright by Andrew Szeto, 2012

DALHOUSIE UNIVERSITY

DEPARTMENT OF ENVIRONMENTAL ENGINEERING

The undersigned hereby certify that they have read and recommend to the Faculty of Graduate Studies for acceptance a thesis entitled "The Investigation of Mysterious Marine Oil Spills on the West Coast of Canada" by Andrew Szeto in partial fulfilment of the requirements for the degree of Master of Applied Science.

Dated: August 3, 2012

Supervisor:

Readers:

DALHOUSIE UNIVERSITY

DATE: August 3, 2012

AUTHOR: Andrew Szeto

TITLE: The Investigation of Mysterious Marine Oil Spills on the West Coast of
Canada

DEPARTMENT OR SCHOOL: Department of Environmental Engineering

DEGREE: MASc CONVOCATION: October YEAR: 2012

Permission is herewith granted to Dalhousie University to circulate and to have copied for non-commercial purposes, at its discretion, the above title upon the request of individuals or institutions. I understand that my thesis will be electronically available to the public.

The author reserves other publication rights, and neither the thesis nor extensive extracts from it may be printed or otherwise reproduced without the author's written permission.

The author attests that permission has been obtained for the use of any copyrighted material appearing in the thesis (other than the brief excerpts requiring only proper acknowledgement in scholarly writing), and that all such use is clearly acknowledged.

Signature of Author

Table of Contents

List of Tables.....	vi
List of Figures.....	vii
Abstract.....	ix
List of Abbreviations Used.....	x
Acknowledgements.....	xii
Chapter 1 Introduction.....	1
Chapter 2 Background Information.....	2
2.1 Ship based oil pollution.....	2
2.2 Marine pollution monitoring and regulations in Canada.....	4
2.3 International efforts at mitigating chronic oil pollution.....	7
2.4 Oil at sea.....	10
2.4.1 The persistence and fate of oil in the ocean.....	10
2.4.2 The modeling of oil at sea.....	12
2.5 Shipping traffic.....	15
2.6 ArcGIS.....	21
2.7 The Analytic Hierarchy Process.....	21
Chapter 3 Research Objective.....	23
Chapter 4 Methodology.....	24
4.1 NASP oil spills and the hindcasting of spills.....	24
4.1.1 Data provided by NASP.....	24
4.1.2 Hindcasting of NASP data.....	26
4.1.3 Ocean Currents.....	29
4.1.4 Wind Data.....	30
4.1.5 GNOME Model Setting.....	31
4.2 Vessel traffic data around spills.....	32
4.3 The identification of possible polluters.....	32
Chapter 5 Results and Discussion.....	40
5.1 The SUR2010060 Spill Event.....	40
5.2 The SUR2010044 Spill Event.....	51
5.2.1 Sensitivity Analysis on the AHP of the SUR2010044 Spill Event.....	57
5.3 The SUR2010075 Spill Event.....	60

5.4	The SUR2010071 Spill Event.....	64
5.5	The SUR2010059 Spill Events.....	69
	Chapter 6 Conclusion.....	81
	References.....	83
	Appendix 1: Wind Data.....	86
	Appendix 2: The SUR2010044 AHP Analysis – Worked out Example.....	95

List of Tables

Table 1. Historic Oil Spills Prosecuted from 1996 – 2000.....	5
Table 2. Summary of Processes Included in Four Models (The Committee on Oil in the Sea, 2003).....	13
Table 3. NASP Data for spills included in the analysis.....	25
Table 4. Saaty's scale of importance (Saaty 1998).....	37
Table 5. Saaty's RI Values (Saaty 1998).....	39
Table 6. Potential Marine Polluter with Criteria Values in the SUR2010060 Spill Event.....	40
Table 7. Categorization of vessels based on time traveled prior to spill detection....	45
Table 8. The Pairwise Comparison of vessels based on hours prior to spill detection.....	47
Table 9. Classification of vessels for distances in area of best guess and uncertainty	48
Table 10. Eigenvectors for distances in the area of best guess and uncertainty.....	49
Table 11. Vessel Rankings in the SUR2010060 Spill Event.....	50
Table 12. Potential Polluters from the SUR2010044 Spill Event.....	53
Table 13. Categorization of the possible polluters in the SUR2010044 Spill Event by time traveled prior to spill detection.....	54
Table 14. The Pairwise Comparison Matrix based on Hours for the SUR2010044 Spill Event.....	55
Table 15. Categorization of the possible polluters in the SUR2010044 Spill Event based on distance in the area of best guess and uncertainty.....	55
Table 16. The normalized results of the AHP process applied to the SUR2010044 Spill Event.....	56
Table 17. Historic Oil Spills (2008-2010) in the Agamemnon Channel.....	62
Table 18. Vessels that passed by the SUR2010071 Spill Event Bounding Polygon.....	68
Table 19. Possible polluters for the SUR2010059_1 Spill Event.....	75
Table 20. Possible polluters in the SUR2010059_2 Spill Event.....	76
Table 21. Criteria Pairwise Comparison Matrix for the SUR2010059_2 Spill Event.....	76
Table 22. Time categorization of the possible polluters in the SUR2010059_2 Spill Event.....	77
Table 23. Classification of possible polluters in the SUR2010059_2 Spill Event based on the distance in the area of best guess and uncertainty.....	77
Table 24. Ranked possible polluters in the SUR2010059_2 Spill Event.....	78

List of Figures

Figure 1. North Adriatic Traffic situation acquired by AIS (Ferraro et al., 2007).....	10
Figure 2. A conceptual model for the fate of oil in the marine environment (ASCE 1996).....	11
Figure 3. CCG AIS Coverage across Canada once AIS reaches full operating capacity (2012).....	17
Figure 4. The LRIT System, showing communication from ship to host and foreign Countries.....	19
Figure 5. A display of the extent of vessel traffic occurring within Canada's Area of Responsibility on a weekly basis.....	20
Figure 6. NASP detected spills analyzed in 2010.....	25
Figure 7. Canadian Terrestrial Weather Stations used for Wind Data.....	31
Figure 8. The SUR2010060 Spill Event Bounding Polygon.....	34
Figure 9. The 'Muskrat', a vessel suspected of polluting in the SUR2010060 Spill Event.....	35
Figure 10. Elements of data and tools used in this Thesis.....	36
Figure 11. Vessel found in the SUR2010060 Spill Event Bounding Polygon.....	42
Figure 12. The structure of the 2010060 AHP.....	43
Figure 13. Potential Polluters in the SUR2010044 Spill Event.....	52
Figure 14. The structure of the SUR2010044 Spill Event AHP.....	53
Figure 15. The MV Frances Barkley.....	56
Figure 16. Normalized ranking of vessels as weight of the distance in area of best guess criteria varies from one to nine.....	57
Figure 17. Normalized ranking of vessels as weight of the distance in uncertainty criteria varies from one to nine.....	58
Figure 18. Normalized ranking of vessels as weight of the time travelled prior to the detection of spill criteria varies from one to nine.....	59
Figure 19. Vessel Traffic around the SUR2010075 Spill Event.....	61
Figure 20. Historic Oil Spills (2008 - 2010) in the Agamemnon Channel.....	63
Figure 21. AIS Coverage from Texada Island and Bowen Island AIS Towers, in relation the the SUR2010075 Spill Event.....	64
Figure 22. The SUR2010071 Spill Event off of Prince Rupert.....	65
Figure 23. Aerial Shot of Prince Rupert that depicts the approximate spill area.....	66
Figure 24. The chronological drift sequence of the SUR2010 at an interval of 3 hours	67
Figure 25. AIS Coverage from Mount Hayes AIS tower in relation to the SUR2010071 Spill Event.....	69

Figure 26. The SUR2010059 Spill Events.....	70
Figure 27. VTOSS Data around the SUR2010059 Spill Events.....	72
Figure 28. LRIT Traffic in and around the SUR2010059 Spill Event.....	73
Figure 29. Potential Polluters in the SUR2010059 Oil Spill Areas.....	74
Figure 30. The vessel track of the radar detected M/T Champion, in relationship to the 2010059 Spill Events.....	80

Abstract

The Government of Canada's National Aerial Surveillance Program (NASP) is responsible for the monitoring of ship based oil pollution in Canada's three oceans. In many of these spills, the source of pollution is unknown as there are often no vessels found in the vicinity at the time of detection. In this work, the oil spills found in 2010 on the West Coast of Canada, alongside the collated vessel traffic data captured by the Canadian Coast Guard are investigated to determine the vessels most likely responsible for these spills. In terms of tools and techniques applied, oil spills are firstly hindcasted using the General NOAA Operational Modeling Environment (GNOME) to determine the location of their source. ArcGIS is used to geospatially reference and combine various data sets, and lastly the Analytical Hierarchy Process (AHP) is used to rank possible polluters found in the area of the spill.

List of Abbreviations Used

AESOP	Adriatic Sea Project
AHP	Analytic Hierarchy Process
AIS	Automatic Identification System
ASA	Applied Science Associates
ASCE	American Society of Civil Engineers
ASP	Applications Service Provider
CCG	Canadian Coast Guard
CEPA	Canadian Environmental Protection Act
CI	Consistency Index
CR	Consistency Ratio
CSA	Canadian Shipping Act
CSN	CleanSeaNet Satellite Services
CSP	Communications Service Provider
DC	Data Centre
DDP	Data Distribution Plan
DRP	Dead Reckoning Position
EC	Environment Canada
EOIR	Electro-optical Infrared Camera System
FA	Fisheries Act
GESAMP	Joint group of Experts on the Scientific Aspects of Marine Environmental Protection
GIS	Geographic Information Systems
GNOME	General NOAA Operational Modeling Environment
GT	Gross Tonnage
HELCOM	Helsinki Commission
IDE	International Data Exchange
IMO	International Maritime Organization
INNAV	Information System on Marine Navigation
I-STOP	Integrated Tracking of Polluters
L	Litre
LE	Lagrangian Elements
LRIT	Long Range Identification and Tracking System
MAN	Manual Tracking
MARPOL	International Convention for the Prevention of Pollution from Ships
MCDA	Multi-Criteria Decision Analysis
MCTS	Marine Communications and Traffic Services
MDA	Maritime Domain Awareness
MMSI	Maritime Mobile Service Identity
MPA	Marine Protected Area
NASP	National Aerial Surveillance Program

NCOM	United States Navy Coastal Ocean Model
NM	Nautical Mile
NOAA	United States National Oceanic and Atmospheric Administration
OCW	Oil in Canadian Waters working group
OSIS	Oil Spill Information System
OSRA	Oil Spill Risk Analysis Model
RDR	Radar
RI	Random Index
SIMAP	The Integrated Oil Spill Impact Model System
SLAR	Side-Looking Airborne Radar
SOLAS	Safety of Life at Sea
TC	Transport Canada
TIN	Triangular Irregular Network
UTC	Coordinated Universal Time
UVIR	Ultraviolet/Infrared Line Scanner
VTOSS	Vessel Traffic Operation Support System

Acknowledgements

I would like to personally thank Dr. Ronald Pelot for allowing me to study under him and helping me out all along the way of this interesting research. Without his keen support and motivation throughout the project, this would have been a much more difficult adventure. The Oil in Canadian Waters research group consisting of Transport Canada, Environment Canada, the University of Calgary, University of Victoria, Mount Allison University and Dalhousie University were key in steering me towards, and aiding me along, this research. In particular, Casey Hilliard from Dalhousie University was extremely helpful with providing the traffic data and the necessary context for this research. Shiliang Shan from the Oceanography Department at Dalhousie University was also very obliging in giving me feedback and manipulating data on various ocean current models and oil drift models that were tested early on in this research. From the United States, Dr. CJ Beegle-Krause from ASA, Bob Simmons (ERDDAP) and Caitlin O'Connor (GNOME) from NOAA were invaluable sources of information for choosing and using oil trajectory models and acquiring the proper data sets from NCOM to feed into these models. Lastly, a very special thank you goes to Director Marc Mes and the Maritime Security group at the Canadian Coast Guard for supporting me both financially and granting me the time off to pursue this research at Dalhousie University.

Chapter 1 Introduction

Ship based oil pollution is an issue that affects the entire globe. While the rare large accidental oil spills are often reported in the news headlines, it is the smaller and much more frequent deliberate and illegal oil spills that are causing an environmental stir all across the world. One of the largest environmental disasters in the United States, the Exxon Valdez oil spill of 1989, resulted in close to 300,000 dead birds found in the vicinity of that spill. In comparison, in Atlantic Canada this is roughly equivalent to the number of dead birds found every year solely due to vessel source chronic oil pollution (Wiese et al., 2001). Here in Canada and in many parts of the world, advanced surveillance using aircraft and satellites to detect polluters is conducted on a regular basis. However a common problem is determining the exact origin of a discharge, one of the many complexities in gathering evidence, such as oil fingerprinting (the comparison of oil from a slick to the oil from a potential source ship). These challenges make it extremely difficult to successfully prosecute these polluters. In this thesis, we use historical spills off the west coast of Canada, detected via the National Aerial Surveillance Program, and hindcast each spill trajectory to find its origin. This spill data is then matched with the Canadian Coast Guard's vessel tracking systems (including Long Range Identification and Tracking (LRIT) and Vessel Traffic Operation Support System (VTOSS)) databases to provide further context for determining the potential sources for each oil pollution event. A methodology is also developed for best identifying these sources of pollution.

Chapter 2 Background information

This chapter reviews the issue of ship based oil pollution, along with existing regulations and means of pollution monitoring in Canada and around the world. The effects of oil at sea are discussed, as well as sources of shipping traffic data that are available in Canada. Lastly the analytic hierarchy process (AHP) is discussed as a means of determining a prioritized alternative when faced with multiple alternatives, each judged using several criteria. AHP is used to determine the most likely polluter in each spill event.

2.1 Ship based oil pollution

Canada is bordered by three major oceans and is home to the world's longest coastline. The oceans support activities including tourism and recreation, fisheries and aquaculture, shipping and transportation, along with offshore oil and gas development. These ocean waters also provide habitat to a wide variety of wildlife such as fish, shellfish, seabirds and mammals that contribute to the economic, social, and environmental well-being of Canadians. Thus our oceans are traversed daily by thousands of vessels ranging from large commercial tankers to small pleasure craft. The steadily growing marine transportation sector is a very effective way to transport goods across the world's oceans and accounts for close to 90% of the entire world's trade (Office of the Auditor General of Canada, 2010). However, marine transportation and other sea-based activities greatly impact the ocean and coastal environments by introducing different types of pollutants. These pollutants are primarily forms of hydrocarbons and their derivatives (Serra-Sogas, 2008).

Oil pollution from these sea-based sources may be accidental or deliberate. Since the introduction of the requirement for a double hull on oil tanker vessels, the volume of oil released during marine accidents (including collisions, fires and groundings) have declined and are continuing to do so (MARPOL73/78). With the introduction of modern vessel safety and collision avoidance tools such as the automatic identification system (AIS), accidental oil pollution has been demonstrably reduced, however it will never be completely eliminated. On the other hand, operation discharges including fuel oil sludge, engine room wastes, foul bilge water (described below), along with the release of oily ballast water and tank washing residues from tankers, account for ongoing deliberate and potentially illegal sources.

In regards to these sources of the operational discharges, when tankers offload cargo and prepare to travel empty, they must take on large quantities of ballast water to maintain the proper balance of the ship. At times, oil cargo tanks and fuel tanks are actually used to hold ballast water and subsequently discharged into the sea when tankers flush out the oil-contaminated ballast water to replace it with new oil (United Nations Environment Programme, 2005). When switching cargoes at port, all tankers have to wash and remove oil residues from hull walls. The remaining residue from tank washings should be stored in tanks called 'slops' and can be discharged only at approved port facilities following strict protocols. However, these rules are not always adhered to and oftentimes this oily mixture is discharged into our oceans.

All types of ships may also discharge pollution into the sea from engine room wastes and bilge waters (interior spillage that collects at the lowest compartment of a ship). In general, this type of waste should be emptied into harbour facilities, however in

practice this does not always happen.

Globally, it has been documented that such deliberate spills have become a regular occurrence and that annually, operational discharges account for 45% of oil inputs to the ocean while shipping accidents account for 36%, and the remainder is from coastal facilities and offshore installation inputs (GESAMP, 2007).

In Canada, these hazards threaten coastal and marine environments. Seabirds are often used as indicators of the state of the marine environment, since the deposits of oil from spills generally form a thin layer on top of the ocean's surface, which coincides with the natural habitat of these birds. Oil tends to stick to the feathers of birds and greatly decreases their insulation, waterproofing and buoyancy, which leads to death from hypothermia and starvation. When oil is ingested, it can damage internal organs. It has been found that even the smallest amount of oil can be lethal to these birds (Wiese et al., 2001). Wiese and Ryan estimates that a minimum of 300,000 birds die every year in Atlantic Canada alone due to vessel source chronic oil pollution. This is approximately the same number of birds killed in the Exxon Valdez tanker oil spill disaster of 1989 in Alaska (Wiese et al., 2001).

2.2 Marine pollution monitoring and regulations in Canada

The international regulation for operational oil pollution from ships is defined in the International Convention for the Prevention of Pollution from Ships (MARPOL 73/78). According to Annex 1 (IMO 1997), the maximum legal operational discharge of oil is 15 ppm per nautical mile operating 50 nm off of any coastline, or not operating in a

designated “special area”, for all vessels types regardless of size and function.

Pollution is banned in designated special areas because they are important either ecologically (marine wildlife in a certain vicinity) or oceanographically (proximity to a coastal areas). However, while these regulations are in place internationally, compliance levels may be as low as 72% (GESAMP 2007).

In Canada, oil pollution crimes are prosecuted under the Canadian Environmental Protection Act (CEPA), the Fisheries Act (FA) and the Canadian Shipping Act (CSA). Under these three laws, the maximum fine for minor offenses is \$250,000 and/or six months in prison for the parties held responsible, and major indictable offenses carry a maximum penalty of \$1 million and/or three years in prison. Under the Canadian Shipping act in particular, Canada was one of the first countries to impose a \$40,000 fine against a polluter caught by aerial surveillance without chemical analysis of oil samples (i.e. comparison of the polluting oil to source oil in the offending ship). From 1996 – 2000 there were 16 cases in Canada, shown in Table 1, in which fines ranging from \$5,000 to \$239,000 were issued for illegal oil pollution (Etkin, 2003).

Table 1. Historic Oil Spills Prosecuted in Canada from 1996 - 2000

Name	Year	Flag	Type	Amount Spilled (L)	Fine (\$CDN)
M/V Atlantic Cartier	1997	Sweden	Container Ship	n/a	\$24,340
M/V Brandenburg	1998	Mauritius	Cargo Ship	n/a	\$36,000
M/V Pine Islands	1998	n/a	n/a	n/a	\$239,00
T/V Nordholt	1998	Liberia	Tanker	n/a	\$40,000
F/V Hogifossur	1998	Bahamas	Research Vessel	100	\$11,300
Sauniere	1998	Canada	Bulk Carrier	37	\$10,000
Orient Tiger	1999	Hong Kong	Tanker	2000	\$8,500
Geco Sigma	1999	Norway	Research Vessel	15	\$5,000
Riverton	1999	Canada	Tug	155	\$5,000

Solborg	1999	Russia	Trawler	50	\$7,500
Ocean Castle	1999	UK	Trawler	100	\$10,000
Polar Duke	1999	Cyprus	Research Vessel	2.6	\$20,000
Atlantic Elm	1999	Canada	Tug	1.26	\$5,000
T/V Nordholt	1999	Liberia	Tanker	15	\$35,000
Orvar	1999	Iceland	Stern Trawler	50	\$6,000
F/V Chokyu Maru	2000	n/a	Cargo Ship	160	\$10,000

*updated successful marine pollution prosecutions may be found at www.marine-pollution-pollutionmaritime.gc.ca/eng/succes_pros/prosectuions/menu.htm

With respect to surveillance, in Canada there are currently three approaches to detecting and deterring illegal oil spills. These are the National Aerial Surveillance Program (NASP), the Integrated Satellite Tracking of Polluters (I-STOP) and in-port inspection programs.

The National Aerial Surveillance Program arose from a collaboration between Transport Canada (TC) and Environment Canada (EC) to detect ship-source oil pollution. While conducting regular, daily aerial surveillance flights to enforce domestic laws and deter potential polluters, NASP also activates mitigation measures for detected spills when warranted. The NASP fleet currently consists of three aircraft strategically placed across the country. These aircraft consist of two Dash-8s and one Dash-7 aircraft, equipped with Side Looking Airborne Radar (SLAR), Ultraviolet/Infrared Line Scanner (UVIR), Electro-optical Infrared Camera system (EOIR), Automatic Identification System (AIS), Satellite Communication Systems and a Geo-coded Digital Camera System. These tools provide several capabilities for detecting marine pollution events and related factors including: the detection of irregularities on the ocean's surface via the SLAR; vessel identification and voyage information via AIS; the capture of still images and video annotated by GPS location data; and high-resolution imagery of marine pollution via the UVIR (Transport Canada, 2010).

I-STOP is also a joint effort between TC and EC. I-STOP serves as a marine pollution early warning system. Using satellite surveillance signals via Canada's Radarsat-2 technology, this program helps direct aircraft to locations of a potential pollution incident in real time. While this is in theory a powerful technique, relevant Radarsat images are few and far between as only three NASP flights have been redirected based on I-STOP warning in the last three 3 years on the west coast of Canada.

This thesis focuses on a problem related to an ongoing collaborative project involving NASP in the Pacific region, thus NASP data from the west coast of Canada will be analyzed in this study.

2.3 International efforts at mitigating chronic oil pollution

Internationally, there are also many initiatives to combat marine polluters. Similar techniques of aerial and satellite detection are used in many places around the world to help prosecute polluters, as the illegal dumping of oil is recognized as an international problem.

In the Baltic Sea, the Helsinki Commission (HELCOM) works to protect the marine environment from all sources of pollution. HELCOM is an intergovernmental co-operation between countries consisting of Russia, Finland, Sweden, Denmark, Germany, Poland, Lithuania, Latvia and Estonia. By orchestrating regular surveillance flights and using satellite surveillance provided by CleanSeaNet (CSN) satellite services of the European Maritime Safety Agency, HELCOM uses a similar approach to that of Canada

to detect illegal polluters. Since the beginning of this program in 1999, the number of deliberate, illegal oil discharges from ships has significantly decreased. In 2010, 149 unreported oil discharges were detected. This accounts for a 70% decline from the figures from a decade earlier. However, of these detected spills, 94% of the illegal polluters remain unknown. This means that only 9 polluters were specifically identified and this appears to be an issue that occurs year-after-year (Stankiewicz et al., 2011).

In the Adriatic Sea, the Italian Coast Guard, working with the European Commission and the University of Ljubljana have conducted similar research. Through the Aerial and Satellite Surveillance of Operational Pollution in the Adriatic Sea (AESOP) project, the main aim is to assess the possibility of setting up a near-real time system using space-borne imagery from Radarsat-1 satellites to support and integrate aerial surveillance of oil pollution. Furthermore, terrestrial AIS traffic information has been archived for the purpose of aiding in the identification of the sources of pollution (Ferraro et al., 2007 and Perkovic et. al 2010).

The two-year AESOP project (2005 - 2006) comprised two phases, in which the first year was dedicated to verification based on the comparison of the results obtained by satellites and aerial and/or naval means over specific and selected geographic areas and fixed periods of time. During the second phase, exercises were run in which space imagery of possible spills were used in near-real time to direct aerial surveillance flights. Preliminary results of the first phase were very positive and encouraged the planning for the second phase. In phase two, satellite images were made available rapidly, however a low number of cases were subsequently verified by

aerial means (where aircraft verify the existence of oil at a spotted site). In the cases in which aerial surveillance was available to verify the existence of oil, approximately 80% of the cases were successfully verified. Additionally, a preliminary examination of the combination of terrestrial AIS was conducted. When this vessel traffic data was overlaid against the spill data, it was recognized that such a combination of information can provide significant added value in determining possible polluters. In the case of one real-time spill, it was found that there were a number of vessels in the vicinity and, under such an event, it was necessary to take into consideration meteorological and oceanographic parameters as well as relevant spill parameters to establish the origin of the spill.

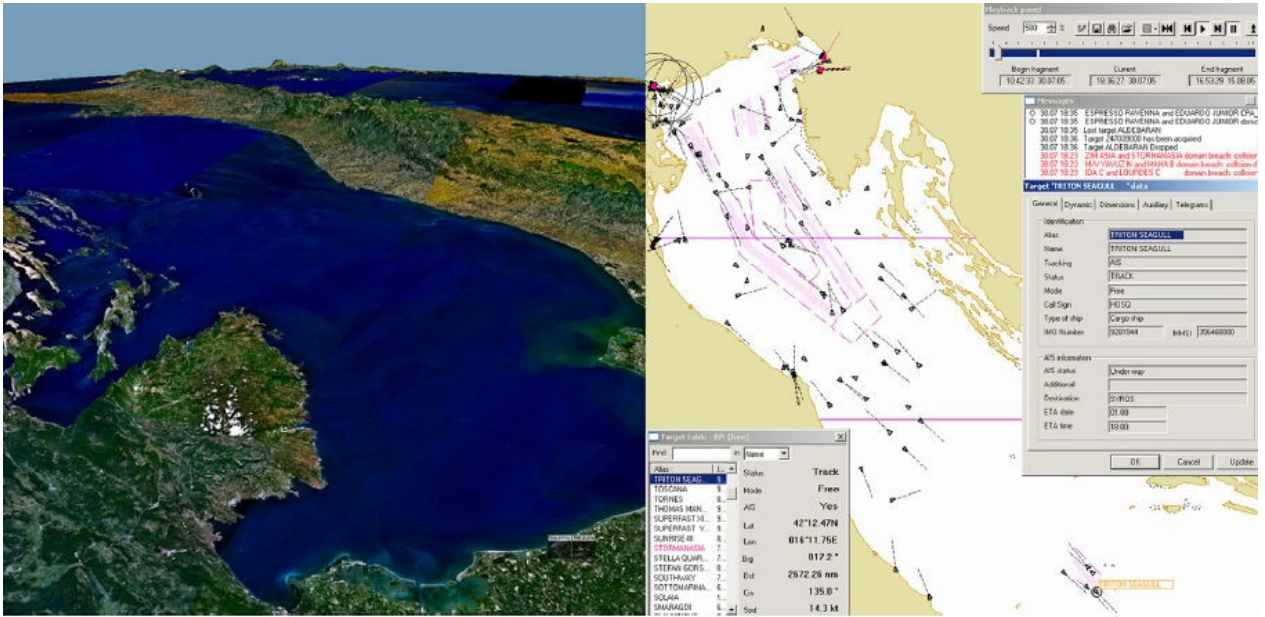


Figure 1. North Adriatic traffic situation acquired through AIS (Ferraro et al., 2007)

The work in this thesis will further the work done by Ferraro and Perkovic. With NASP flight data and vessel traffic information from the Canadian Coast Guard, a similar approach will be taken to determine the gravity of the situation here in Canada, and to provide a systematic way of determining the most likely polluter in the case of a spill.

2.4 Oil at sea

This section describes the effect of oil in the ocean and how the transportation of oil on the surface of the ocean can be modeled.

2.4.1 The persistence and fate of oil in the ocean

Oil spilled in the ocean is subject to: advection (the transport mechanism of a substance)

due to currents and wind; horizontal spreading due to turbulent diffusion; various mass transfer processes; and change in physicochemical properties of the oil due to weathering processes such as evaporation, dispersion and dissolution. Figure 2 shows these various processes that may occur to the oil in ocean.

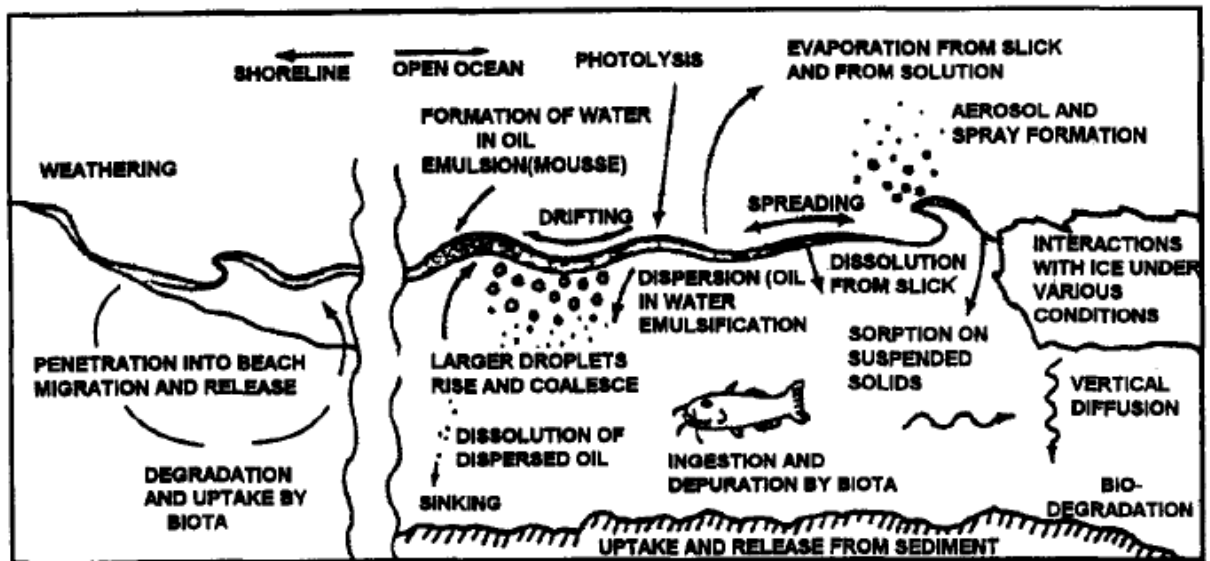


Figure 2. A conceptual model for the fate of oil in the marine environment (ASCE 1996)

Weathering is an important factor in the behaviour of spills. As the oil is deposited on the water it begins almost immediately to transform the oil into substances with different physical and chemical characteristics from its original form. Evaporation alone is one of the most important processes for spill dynamics as within a few days of a spill, light crude oils will lose up to 75 percent of their initial volume and medium crudes will lose upwards of 40 percent (The Committee on Oil in the Sea, 2003). However while it is understood that weathering is important for determining the status of the spill, for the types of situations examined in this thesis, the oil is often weathered by the time it is detected, however associated characteristics are not recorded. Since information about the spill at its origin is generally unknown, any analysis based on the fate of the oil becomes extremely difficult and is thus ignored in this work. The surface transport of the

oil is the primary focus of this thesis when determining the origin of these spills.

The process of advection is the main physical process that governs the drifting of a surface oil spill. Advection of oil is caused by the effects of surface currents and wind on the oil. Given that most oil spills are initially buoyant and float on the surface of the ocean, their transport is dominated by surface currents, which is the continuous directed movement of ocean water and the dragging of the oil from local winds. In regards to the transport speed of slicks on the ocean's surface, it has been observed that this typically varies from 2.5% to 4.4% of the wind speed, with a mean value of 3.0 – 3.5%. The deflection angles vary between 0 and 25% to the right or left of the wind direction with a mean value of 15% (ASCE 1996).

2.4.2 The modeling of oil at sea

A variety of oil spill models are readily available for the forecasting of marine oil spill trajectories in the world today. While there are many complex models that support both the 2-D transport of oil across a surface and 3-D transport of oil throughout the water column, given our scenarios this research requires a 2-D model. In table 2, the third edition of Oil in the Sea report (The Committee on Oil in the Sea, 2003) provides a summarized comparison of four widely used models.

Table 2. Summary of Processes Included in Four Ocean Current Models (The Committee on Oil in The Sea, 2003)

Process	GNOME	OSIS	OSRA	SIMAP
Dimensions	Near-surface	Near-surface	Near-surface	Entire water column
Advection	Wind factor + background current + stochastic uncertainty	Wind factor + background current + wave	Wind factor + background current	External hydrodynamic model + wind factor (if not in hydro model)
Spreading	Modified Fay + Wind Component	None	None	Modified Mackay et al. (1980)

These models however were created for different purposes. The Oil Spill Risk Assessment Model (OSRA) was developed by the Minerals Management Services in the United States and is used to estimate spill impact associated with offshore oil development in the Outer Continental Shelf of the United States. With a fairly specific purpose and inability to perform post-spill trajectory modeling in comparison to the other models, it was disregarded for this research. The Integrated Oil Spill Impact Model System (SIMAP) is a commercial product developed by Applied Science Associates (ASA) in the U.S. primarily for strategic planning of resource allocation in the event of a spill as well as post-spill analysis. It differs from the rest of these models because it is capable of modeling oil dispersion over the entire water column. The Oil Spill Information System (OSIS) is another commercial product developed by BMT Group Ltd., and is more frequently used in Europe. However these commercial tools cost upwards of \$10,000 and lack the necessary baseline data sets for the intended area of interest. Lastly, the National Oceanic and Atmospheric Administration (NOAA), which is primarily responsible for providing spill modeling expertise to the U.S. Coast Guard, has

developed the General NOAA Operational Modeling Environment (GNOME), which accounts for advection, spreading and first order evaporation. A major advantage of this model is that it has been tested and used within North American waters. Also with this tool being free and leveraged by our Canadian government counterparts in the United States, this makes this particular model a good fit for this research.

GNOME is the primary tool applied by NOAA to the analysis of major oil spills over the past decade. It is a standard Eulerian/Lagrangian spill-trajectory model (where specification of the oil spill is represented by individual oil particles' behaviour) providing the *best guess* trajectory of where a spill will go, and its *uncertainty bound*, better known as 'minimum regret' in the system. Modelers can use GNOME in its Diagnostic mode, where custom trajectories can be produced for spill events anywhere around the world. For example, in regards to the Deepwater Horizon drilling platform spill in the Gulf of Mexico in 2010, even though it was primarily a subsurface spill, GNOME was used to track the surface slick to forecast the beaching of oil. GNOME proved to be fairly accurate for this spill and has been documented as providing accurate results elsewhere around the world (Cheng et al., 2011). Using a combination of user-supplied information on local ocean winds, currents and oil characteristics, GNOME is able to estimate oil spill movement through analyzing wave stress, wave compression, Stokes drift, dispersion, over-washing, surface drift and Langmuir circulation (Beegle-Krause, 2001). Once the oil spill movements are calculated, GNOME also allows for conversions of its output to ArcGIS-ready formats.

In the present work, GNOME will be used to simulate the hindcast of the NASP

detected spills. The model settings, along with the currents and wind forcing data, will be discussed in the methodology section.

2.5 Shipping traffic

Shipping traffic data analyzed in this thesis is supplied by the Canadian Coast Guard. The Coast Guard runs 22 Marine Communications and Traffic Services (MCTS) centres across the country, which are responsible for monitoring all vessel traffic in Canada. These centres provide communications and traffic services to the maritime community for the purposes of safety of life at sea, in accordance with international agreements. Specifically, in this work two sets of traffic data are used: Vessel Traffic Operations Support System (VTOSS); and Long Range Identification and Tracking (LRIT) System.

VTOSS is a set of software program modules developed by the Coast Guard in Vancouver to support marine traffic regulations of various communities, harbours and inlets located on the Pacific coast. Until 2011, it served as the primary day-to-day vessel monitoring tool for MCTS and also stored all vessel data and activity in a central database. While this system has been recently decommissioned, its vessel traffic information is still relevant and is actively fed to the current Information System on Marine Navigation (INNAV) for the same purposes. Within VTOSS, most ships that are twenty meters or more in overall length or every ship engaged in towing or pushing any vessel or object, was tracked. Exceptions include pleasure yachts less than thirty metres, and fishing vessels less than twenty-four metres in

length and less than 150 tons (Perret, 2003).

Vessel positions were collated from four major sources. These sources include radar tracking, Automatic Identification System (AIS) tracking, dead reckoning and manual tracking.

Radar tracks were stored and displayed in real-time from radar systems deployed along the coast. A radar system is an accurate way of determining ship position, however these systems were primarily placed along the Strait of Juan de Fuca which leads into Vancouver. With radar, a vessel's identity is not readily available to the operator, however the acquisition of the vessel identification through other systems was generally possible and this information was regularly appended to these tracks either automatically after initial tagging, or based on the experience of on-shift MCTS officers. This method proved to be very successful and fairly accurate for the purposes of MCTS (Perret, 2003).

In 2000, the International Maritime Organization (IMO) introduced mandatory carriage of AIS for merchant vessels in an amendment to the Safety of Life at Sea (SOLAS) convention, coming into force by 2004. The regulation makes AIS mandatory for all merchant ships of at least 300 gross tonnage (GT) conducting international voyages, cargo ships of 500 GT and upwards not engaged in international voyages, and all passenger ships irrespective of size. AIS transmits a variety of different data, including a ship's IMO number, Maritime Mobile Service Identifier number (MMSI), ship name, bearing, speed, ship type, ship length, ship width and position, to other ships and to shore stations. The Canadian Coast Guard

owns one of the most comprehensive networks of AIS shore-based systems in the world, detecting vessels over 40 nautical miles (nm) away from its shores. These shore-based systems receive dynamic position reports from all AIS compliant vessels at rates up to every 15 seconds. Figure 3 shows the Coast Guard AIS coverage when full operating capacity will be met in 2012. The green polygons represent an approximate range of 40 nm from each terrestrial station.



Figure 3. CCG AIS Coverage across Canada once AIS reaches Full Operating Capacity (2012)

Dead Reckoning is incorporated as a plotter module within VTOSS. The vessel is tracked by choosing a series of selectable waypoints and entering transit speed or estimated time of arrival. The vessel track then automatically follows the predetermined route calculated by the software. These positions are reasonably accurate, but precision

depends on the accuracy of the starting points supplied by the vessel (Perret, 2003). Given the pervasiveness of modern tracking techniques (i.e. AIS and LRIT), the dead reckoning method is quickly becoming a secondary tracking method.

Manual tracking is another form of vessel reporting from VTOSS. This is done by selecting a vessel's icon and dragging it on the monitor in real-time to its new assumed position. This is generally the least exact position source data (Perret, 2003).

In May of 2006, The Marine Safety Committee adopted a new SOLAS Amendment on Long Range Identification and Tracking (LRIT) of vessels. This amendment to SOLAS Chapter V requires that ships be fitted with equipment to transmit the LRIT information automatically (ship's ID, position, date/time of position). Similarly to AIS, passenger ships, high speed craft, mobile offshore drilling units and cargo ships of 300 gross tons and upwards are regulated to comply with the system by the 160 Contracting Governments of the IMO. Currently, this system has become fully operational and has been implemented in many federal departments across Canada for the purposes of maritime security, safety, environmental response and search and rescue.

The Canadian Coast Guard, through its Maritime Security directorate, is the lead agency providing LRIT data and managing the system in Canada. LRIT serves as a worldwide satellite-based tracking system that uses existing ship-borne equipment to track SOLAS-class vessels on international voyages. The underlying principle is that positional data and other tombstone (i.e. flag, vessel name, etc.) LRIT information from tracked vessels are transmitted from ship-borne equipment to the

Data Centre (DC) of the Government whose flag that ship is flying. Other governments wishing and entitled to receive these data for maritime domain awareness (MDA) must make a Port or Coastal request from their own DC, through the International Data Exchange (IDE), to the flag's DC. Unlike AIS, LRIT is a secure point-to-point system, in which each administration retains rights to its own flag data. Figure 4 is a depiction of the flow of information from ship to another country's data centre and users. In this figure, CSP and ASP stand for Communications Service Provider and Application Service Provider, respectively. CSPs generally consist of satellite companies providing the data link, and ASPs are the user interfaces. The DDP represents the Data Distribution Plan that stores each flags' area of entitlement (1000 nm from a nation's coastline).

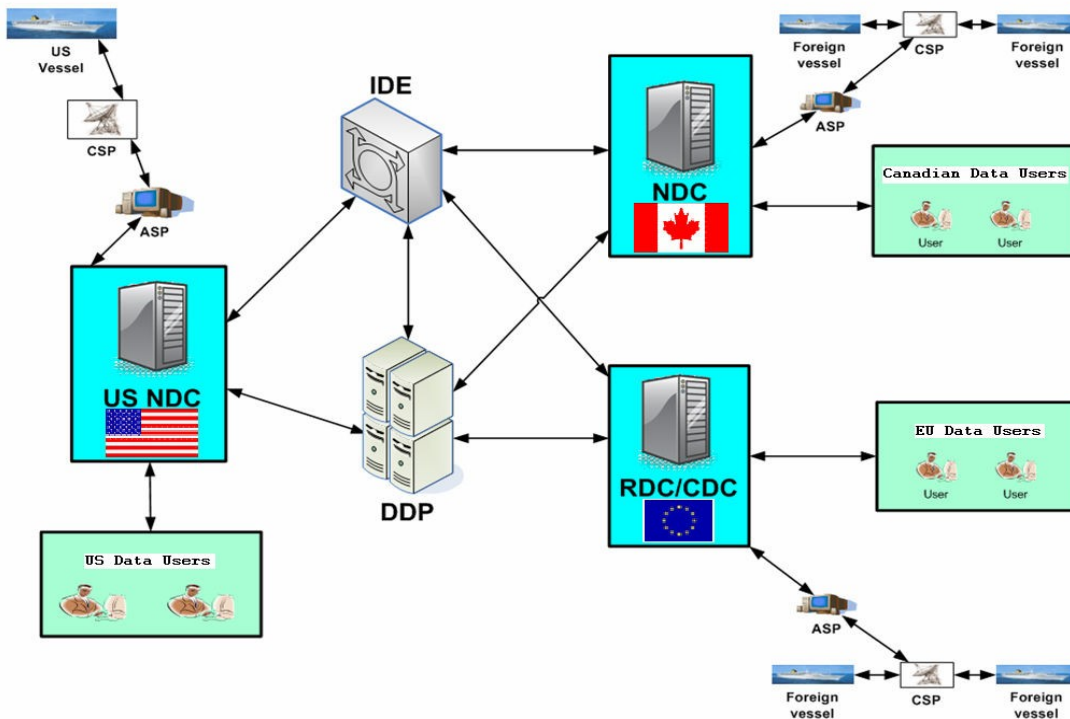


Figure 4. The LRIT System, showing communication from ship to host and foreign countries. (Canadian Coast Guard)

Within the Canadian LRIT system, Canadian flagged vessels all around the world, foreign vessels intending to come into Canadian ports, and all vessels within 1000 nm of Canadian shores (Canada's Area of Responsibility) are tracked in real-time. The system currently tracks up to about 900 vessels a day within the Canadian area of responsibility.

LRIT vessel information includes a timestamp, latitude, longitude, vessel name, IMO number, MMSI number and flag. Positions are reported automatically at a standard rate of once every six hours (4 times a day), however they can be requested by the vessel's flag country or by a country whose waters the vessel traverses, to report more frequently, up to once every 15 minutes.

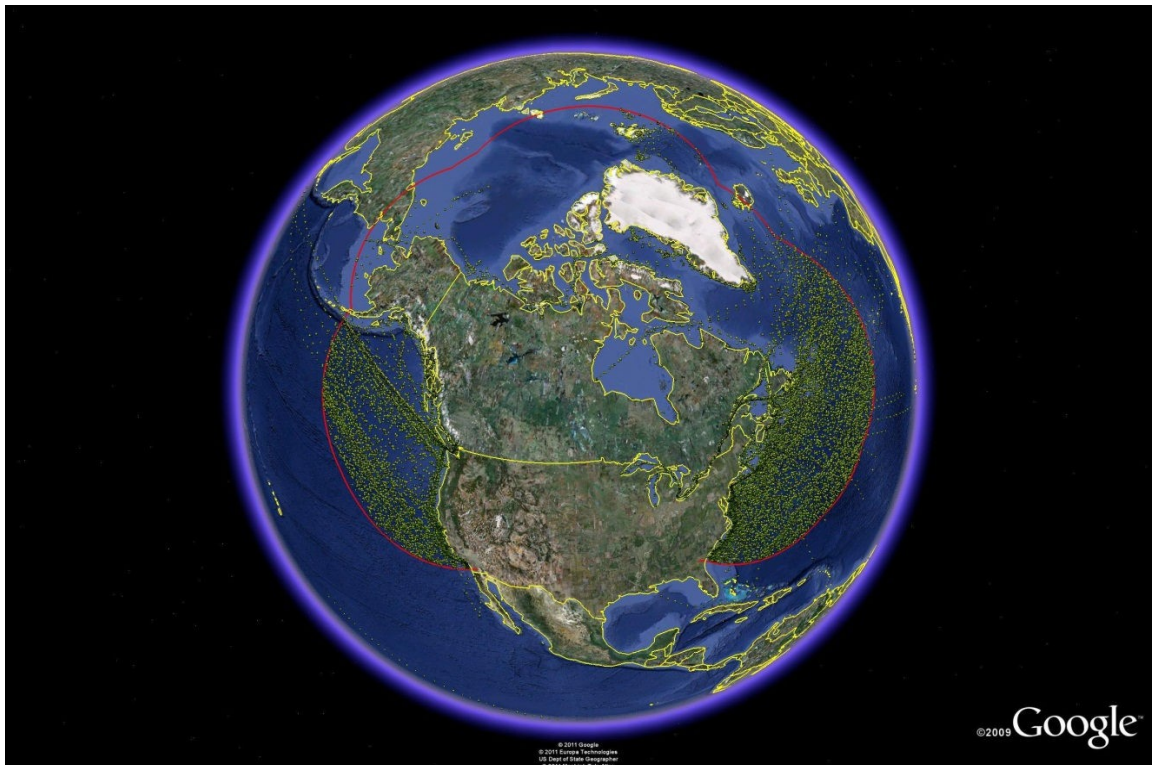


Figure 5. A display of the extent of vessel traffic occurring within Canada's Area of Responsibility on a weekly basis

While other ship tracking systems such as shore-based AIS are capable of tracking SOLAS class vessels out to approximately 40 nm from Canadian shores, LRIT is meant to complement this system, having a range out to 1000 nm. With over 80 nations contributing to LRIT, this tool is widely recognized as a valuable global maritime traffic monitoring system (Hoye et al., 2008). In this research, LRIT traffic is used to analyze two offshore spills, however inshore the density of other vessel traffic sensors prove to be much more useful in analysis, thus LRIT is not used in these instances.

2.6 ArcGIS

In this work, ArcGIS is the geographic information system (GIS) software used for the purposes of geospatial analysis of both vessel traffic and hindcasted oil spills. ArcGIS was created by ESRI and is used for creating and using maps, compiling and analyzing geographic information. In Canada, in the maritime domain, the Canadian Coast Guard uses ArcGIS version 10, for the purposes of historical trend analysis on domestic vessel traffic, along with the tracking of the Coast Guard's fleet. Thus ArcGIS version 10 is used in this research.

2.7 The Analytic Hierarchy Process

The Analytic Hierarchy Process (AHP) is a method used to evaluate and rank options when faced with multiple criteria. This technique is a part of a larger family of decision aids, known as Multi-Criteria Decision Analysis (MCDA). MCDA provides a systematic methodology that can be used to quantify weighted criteria across a set of alternatives. The use of MCDA in the environmental sciences has grown in the past few decades as these methods have shown significant improvements in decision processes (Huang et.

al, 2011). While most of the popular MCDA techniques share similar mathematical elements, the AHP technique is by far the most commonly used in environmental science and has yielded successful applications, particularly in the Geographical Information Systems (GIS) world (Huang et. al, 2011). Created by Thomas Saaty in 1977, AHP is an approach that utilizes a series of pairwise comparisons of criteria to ask, "how much more important is one option than the other?". In the marine world this technique has been used in the United Kingdom to provide performance indicator importance for Marine Protected Area management (MPA) (Himes, 2007). Amongst a variety of stakeholder groups, AHP was used to prioritize performance indicators to better understand the needs and interests of these groups when developing management strategies for a MPA. In Croatia, AHP has been used with GIS to find the most desirable location for a ship to take refuge in the case of an environmental hazard (Bradaric et. Al, 2008). From these examples, AHP was flexible in defining and weighting criteria, along with being simple to use in ranking alternatives. These traits made this tool clearly stand out as the tool to be applied in this particular study. In this thesis, as oil spills are historically drifted and as vessel traffic has been analyzed against these spills, the AHP is required for analyzing the many different criteria for finding the most likely polluter in each of the reported spill scenarios.

Chapter 3 Research Objective

- The purpose of this research is to determine the most likely polluters in “mystery” oil spill events, where the event has been detected but the culprit is unknown. In Canada, with the availability of comprehensive vessel traffic data and a national surveillance program to detect these types of spills, a logical step would be to combine these two elements to determine who the most likely polluters are, which will help for future oil spill prevention and response planning. The overall objective in this work is to combine vessel traffic information with detected oil spills from 2010 on the West coast of Canada, and to develop a methodology for determining the most likely polluter in these spill events. Sub-objectives of this work include:
 - Determining what drift model best represents the historical spill trajectory for these spill events.
 - Given multiple available datasets of vessel traffic, determining the best vessel traffic set to be analyzed in different spill events (VTOSS versus LRIT).
 - Establishing a methodology to suggest the most likely polluter amongst many possible culprits based on multiple criteria available in each spill event.

Chapter 4 Methodology

This section describes in detail the tools and techniques used in this thesis, from analyzing oil spills to overlaying vessel traffic information for the purposes of determining the most likely polluter in a spill event.

4.1 NASP oil spills and the hindcasting of spills

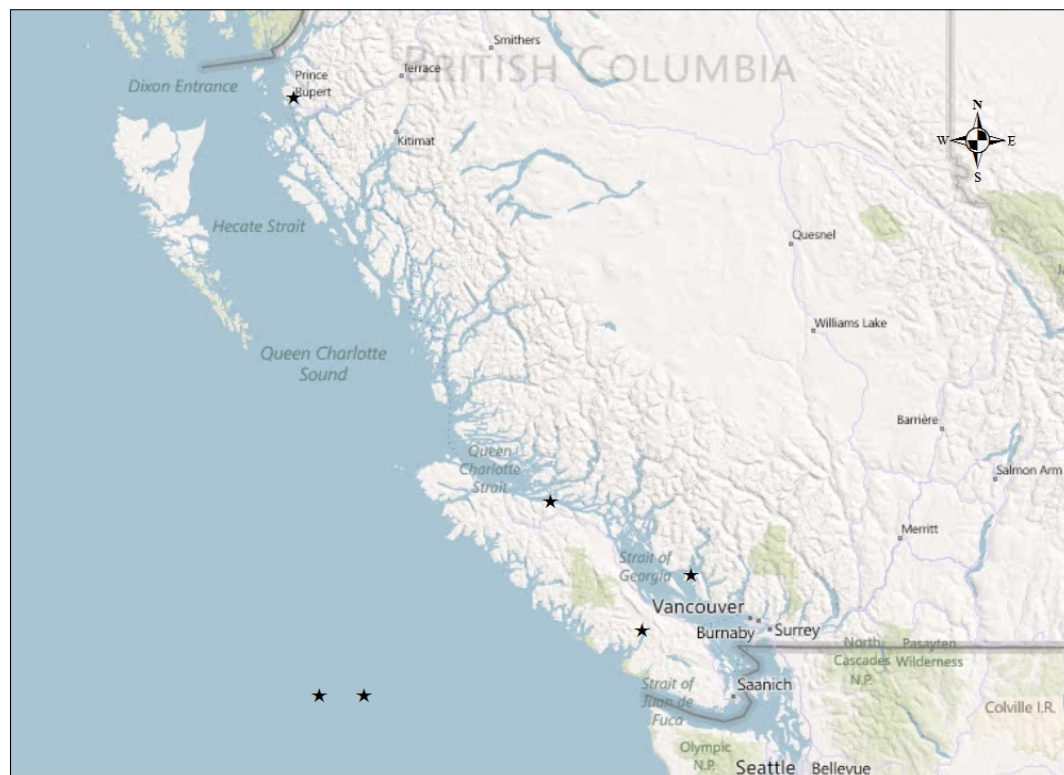
This section covers the data provided through the National Aerial Surveillance Program, the hindcasting of oil spills using 2-D modeling tools, as well as specific settings needed for these models.

4.1.1 Data provided by NASP

The data provided by NASP that are analyzed in this research are the spills from the West Coast of Canada in 2010. While oil spill data sets exist for the Pacific, Arctic and Atlantic oceans, the Pacific data set was analyzed in depth as the Pacific Region NASP was an integral partner in this research, and since adequate vessel traffic data was available in this particular area. Of the spills during this time period and in this region, data on 10 spills from both offshore and inshore were provided. Four of these spills were detected in port facilities hence were not analyzed since they did not occur during vessel trips, while the remaining six spills were analyzed. The average size of the analyzed spills was 104 litres per spill event. Data recorded from each observed spill included the NASP flight number, spill latitude/longitude, date, time, and estimated spill volume. The raw data from these observations are shown in Table 3. Figure 6 shows where these six spills were located.

Table 3. NASP Data for spills included in the analysis.

Flight #	Date	Time (UTC)	Source	Volume (L)
SUR2010044	6/23/2010	21:00	Mystery	13.2
SUR2010059	7/29/2010	18:45	Known	97
SUR2010059 (2)	7/29/2010	17:44	Known	195
SUR2010060	8/24/2010	19:15	Mystery	18.61
SUR2010071	10/28/2010	21:49	Mystery	300
SUR2010075	11/03/2010	21:06	Mystery	2.11



60 30 0 60 Nautical Miles



Legend

★NASP Detected Spill selection

Figure 6. NASP Detected Spills in 2010 for Analysis

In this thesis, the separate flights (by flight number) will be used to help identify each spill event and the vessel traffic around these spills.

4.1.2 Hindcasting of NASP data

In NASP's reporting of these oil spills, there is no estimate of the time of the spill initiation and there is no official weathering status on the oil. Thus a viable approach is to use a 2-D horizontal trajectory model to investigate the historical horizontal movement of the oil through spreading, advection, dispersion and entrainment. As advection is the main mechanism governing the location of the oil following discharge due to the effects of surface currents and wind drag on oil, a 2-D trajectory model analyzing the surface currents, winds and wave fields is well-suited. This is also reasonable since most oils are initially buoyant and float on the sea surface (ASCE 1996). Given the 600 over-flight hours a year, the common flight patterns are re-flown once every few days, thus there is little time for these surface slicks to go unnoticed or weather away dramatically.

As noted in section 2.4.1, light crude oils can lose up to 75% of their initial volume and medium crudes up to 40% within the first few days following a spill (The Committee Oil in the Sea, 2003). With the overflight patterns performed by NASP (which re-fly a similar pattern every 2-3 days), it is assumed that most slicks do not go unnoticed for extended periods of time (several days). Lastly with the spills best classified as "light crudes" by NASP, it was decided that a three-day hindcast is sufficient to help determine the source of these oil spills, using the GNOME oil trajectory model. Furthermore, in regards to comments made in section 2.4.1 about using non-weathering oil, the oil type used in GNOME does not have an effect on the actual horizontal transportation of the oil.

GNOME is a standard Eulerian/Lagrangian spill-trajectory model. To represent an oil spill, GNOME uses Lagrangian/Eulerian elements (LE) which are called 'spots' in the

tool. These plots are a collection of point representations that collectively represent the extent of a spill. The black splots represent the *best guess* scenario while the red splots represent a minimum regret or *uncertainty bound*. These splots move within continuous flow fields to provide trajectory modeling, according to equation 1.

$$\frac{dC}{dt} = -(V * \nabla)C + (k\nabla C) + S \quad (1)$$

where C is the mass concentration of the pollutant, V is the advective velocity of the surrounding medium, ∇ is the gradient operator, k is the turbulent diffusion tensor and S is the sink or source term in relation to time, t.

The above equation essentially represents the time rate of change of the oil concentration at any location, (dC/dt) , due to changes caused by currents moving it around, $[-(V * \nabla)C]$, diffusion spreading it out, $(k\nabla C)$, and sources that add pollutant at some point in time and location (S). The parameters for the three terms on the right-hand side of this equation are based on either model predictions or algorithmic formulas that are independent of the equation (1), thus they enter into the equation as external parameters (Galt 1997).

GNOME uses the data to simultaneously run separate separate spills using individual LEs to sample the uncertainty over the spill's trajectory. Each of these uncertainty elements (depicted as red splots) sample a different portion of the uncertainty space. For example, one splot may result from faster winds that are headed more to the westward direction, a smaller diffusion, and slightly slower currents. Another uncertainty element might have slower winds, a much larger diffusion, and faster currents slightly towards the eastward direction. The trajectories of these uncertainty LEs map the domain for the minimum regret solution and are used in GNOME to calculate an

uncertainty boundary for the slick trajectory. Quantitative confidence limits are not available, but this uncertainty bound combined with the *best guess* solution has generally been considered a 90% confidence limit based on experience (Beegle-Krause, 2001). In most spill events, the *uncertainty* LEs are used by responders to examine potential spill trajectories and ascertain the degree of protection required for highly valuable or vulnerable receptors. The main difference between the best guess and minimum regret solutions, are that while minimum regret will less likely identify the exact position, when used in the forward direction it exposes potentially dangerous or expensive resources that may be affected. In the backwards or hindcast direction as in this work, it represents possible areas with which the pollution may have originated. If all the vector transport and dispersion processes are represented by the deterministic forecast values plus a random component that realistically spans the errors, then the statistical ensemble will cover the uncertainty that is likely in the forecast (minimum regret), which is consistent with a Monte Carlo representation of a first-order error analysis applied to a deterministic forecast (Galt 1997).

The turbulent diffusive transport is also another mechanism accounting for both the lateral and vertical shear that is accounted for in GNOME. This allows for oil slicks to elongate in the direction of wind and waves. Classically, this is calculated by a random walk procedure with a user-specified horizontal diffusion coefficient in the range of 1-100m²/s (ASCE 1996). The diffusive velocity is then calculated by equation 2:

$$V_d = \sqrt{4 * D_h / \Delta t_p} \quad (2)$$

where V_d is the diffusive velocity, D_h is the diffusion coefficient in the horizontal plane (in m²/s) and Δt_p is the time step (Cekirge, et al., 1995). With this in mind, the challenge becomes hindcasting these spills to determine the historical trajectory. This modeling is described in the section to follow.

4.1.3 Ocean Currents

The reliability of oil trajectory models are critically dependant of the quality of the environmental parameter inputs. Ocean currents are an important element as this ultimately determines where the oil may end up, or in our case, where it came from.

There are four methods for obtaining advective currents. These methods include using current atlases that describe the nature of the currents in a particular region, deriving them through terrestrial or satellite radar measurements, measuring them by the activity measured in surface drifting buoys, and producing them through hydrodynamic models.

In Canada, the Canadian Hydrographic Service (CHS) has produced an atlas of tidal currents, including the hourly velocity and direction of tidal currents since 1995, according to provisions in the Canadian Shipping Act. These records are available by region and organized by year on the CHS website. These records are specific to particular monitoring stations in each region (Arctic, Atlantic, Great Lakes, Hudson Bay, Pacific and St. Lawrence) but are only available as static atlases, from authorized chart dealers. This makes these charts difficult to use in assessing oil spills, particularly for the purpose of implementing them in real-time (CHS, 2010).

Depicting currents by high frequency remote radar sensing is another technique to gather ocean current data. This technique is particularly useful close to shore, in estuaries and around bays. This technique provides the highest spatial resolution, as fine as a few hundred meters. Used primarily for search and rescue operations, oil spill response, coastal navigation, near shore engineering projects and environmental modeling, this technique is used for specific tasks and is not readily-available on a daily basis (OEA Technologies, 2011).

In terms of using marine buoys for providing surface currents data, Canada has a

network of buoys providing wind speed, wave height, wave period, air temperature and water temperature, but does not have the capability to provide currents data (Environment Canada, 2010).

Since the first three methods do not provide all the information required for analysis, the use of a hydrodynamic model was employed as they are generally widely used and are relatively easy to apply (Reed et al, 1999). In this work, global ocean currents are obtained from the US Navy Research Laboratory's, 3-D Navy Coastal Ocean Model (NCOM). The spatial resolution of NCOM is $1/8^\circ$ and temporal resolution is 3 hours. The time variation of currents are calculated based on start time and the run duration that are entered into GNOME. A 3-day period prior to the spill is used to initiate the simulation.

4.1.4 Wind Data

As described in section 2.4.2, surface winds are an important parameter to be used in the modeling of the oil spills. In Canada, hourly historical wind data are harder to acquire from sea-based sources since Environment Canada does not appear to store data from their offshore buoys. Thus hourly wind measurements from terrestrial stations including Port Hardy, Campbell River, Tofino and Vancouver are used as shown in Figure 7. Values used for the forcing the GNOME model are tabulated in Appendix 1.

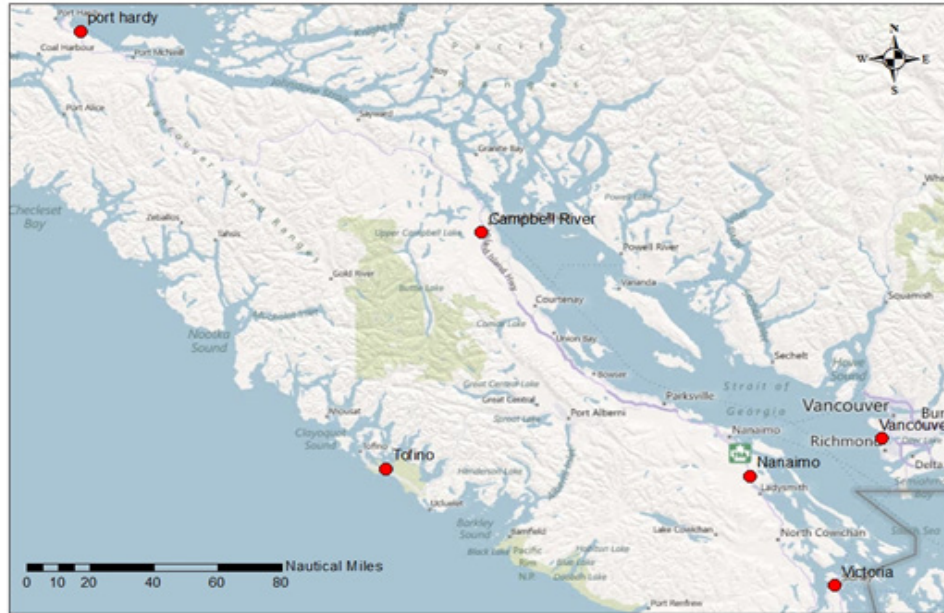


Figure 7. Terrestrial Weather Stations used for Wind Data Sourcing

4.1.5 GNOME Model Setting

In GNOME, the diagnostic mode was used, in which full manipulation of the tool, including geographical location, and inputted wind and currents data was possible. By running the tool in reverse temporal mode, a hindcast of a spill was produced. When running the tool, the user must have an idea of the temporal scales involved to appropriately set up the model.

Due to the uncertainty of the ocean currents, GNOME was run with a minimum uncertainty error of 10% for ocean current speeds in both along-current and cross-current directions, which was consistent with Cheng’s work in 2011. In GNOME, 50 barrels or 7.95 m³ of oil is equivalent to 200 splots (Cheng et. al., 2011). Thus on average about 10 splots were used to represent each of the spills in this research. GNOME simultaneously uses an additional 10 red splots to sample the uncertainty bound.

For the calculation of how oil spreads horizontally, this is simulated by the random walk

effect, where users input a diffusion coefficient which is used to calculate random step lengths in the x and y directions from a uniform distribution (Beegle-Krause, 2001). In this work, the value of the diffusion coefficient and its uncertainty factor are set as 100,000 cm²/s⁻¹ and 1, respectively which are default values used by Cheng for the Deepwater Horizon spill (Cheng et. al, 2011).

Once these LEs have been drifted, a recommended approach to better analyze the trajectory is by using the points as vertices for a Delaunay triangulation. These representations are calculated via a triangular irregular network (TIN). By representing the spills in this manner the bounding polygons created the TIN are used as possible areas of discharge as opposed to individual spill elements. This is done in ArcGIS as hourly plot files were available for import into ArcGIS.

4.2 Vessel traffic data around spills

VTOSS traffic data was used for four of the six spill events. VTOSS was used in preference over LRIT in these four spills as it provided dense traffic data (multiple positions per vessel per minute) which allowed for a comprehensive study. Offshore, the recorded traffic in VTOSS was sparse as it was beyond the spatial scope of MCTS, thus LRIT provided the main coverage there.

As LRIT became operational and reliable by 2010, LRIT data was used in analyzing the two -SUR2010059 offshore spill events.

4.3 The identification of possible polluters

For each spill event analyzed, 24 plot files, at 3 hour intervals over 72 hours, were

imported into ArcGIS to develop a bounding polygon to find vessels transiting around the area of the spill. For example, Figure 8 is the bounding polygon for the SUR2010060 spill event. As mentioned in Section 2.6, ArcGIS version 10 is using the World Geodetic System 1984 geographic coordinate system.

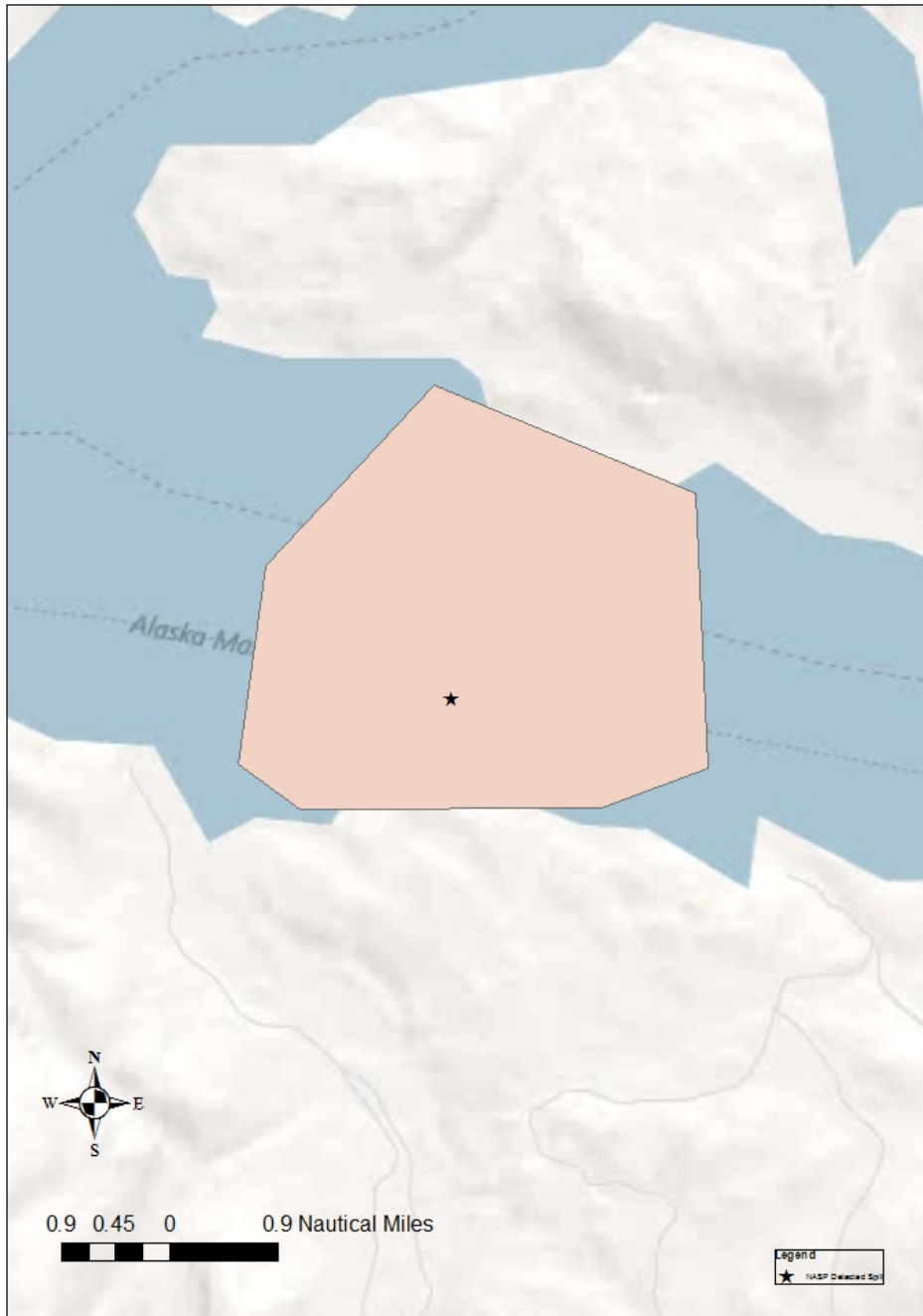


Figure 8. The SUR2010060 Spill Event Bounding Polygon

Vessel tracks found in these bounding polygons would then be clipped (using an ArcGIS tool to extract input features, which in this case are the vessel trajectories that overlay the bounding polygon for an oil spill) to establish a list of possible polluters. Each vessel was then plotted temporally against the nearest hourly polygons (*Best Guess* and *Uncertainty*) at the time at which they would have passed through the area of the spill. For instance in Figure 9, the circles represent the 'Muskrat', a vessel that traversed the area of the oil spill 24 hours prior to spill detection in the SUR2010060 spill event. Thus the 'Muskrat' was plotted against where the oil spill would have most likely been 24 hours prior to the detection of the spill.

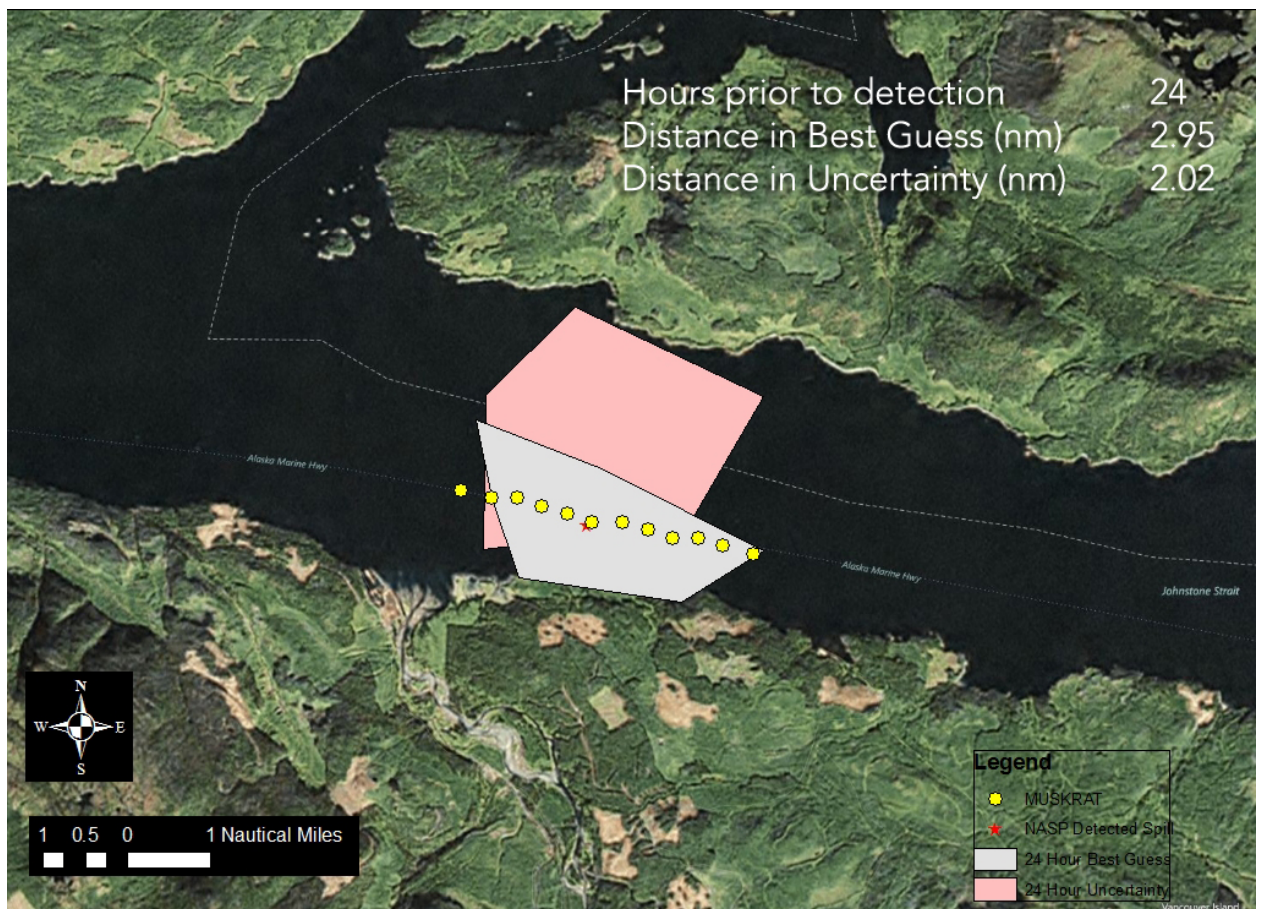


Figure 9. The 'Muskrat', a vessel suspected of polluting in the SUR2010060 Spill Event

In figure 9, the Muskrat is plotted against the polygons for the area of *best guess* and *uncertainty*, where its distance across each of those two polygons is determined in ArcGIS.

With the possible polluters identified for each spill event classified according to the time with which they passed through the area of the oil spill prior to the detection of the spill by NASP, the distance spent in the area of *best guess* of the spill and the distance spent in the area of *uncertainty* for the spill, the multi-criteria decision analysis tool AHP was then used to rank these vessels. Figure 10 shows the overall workflow of this thesis.

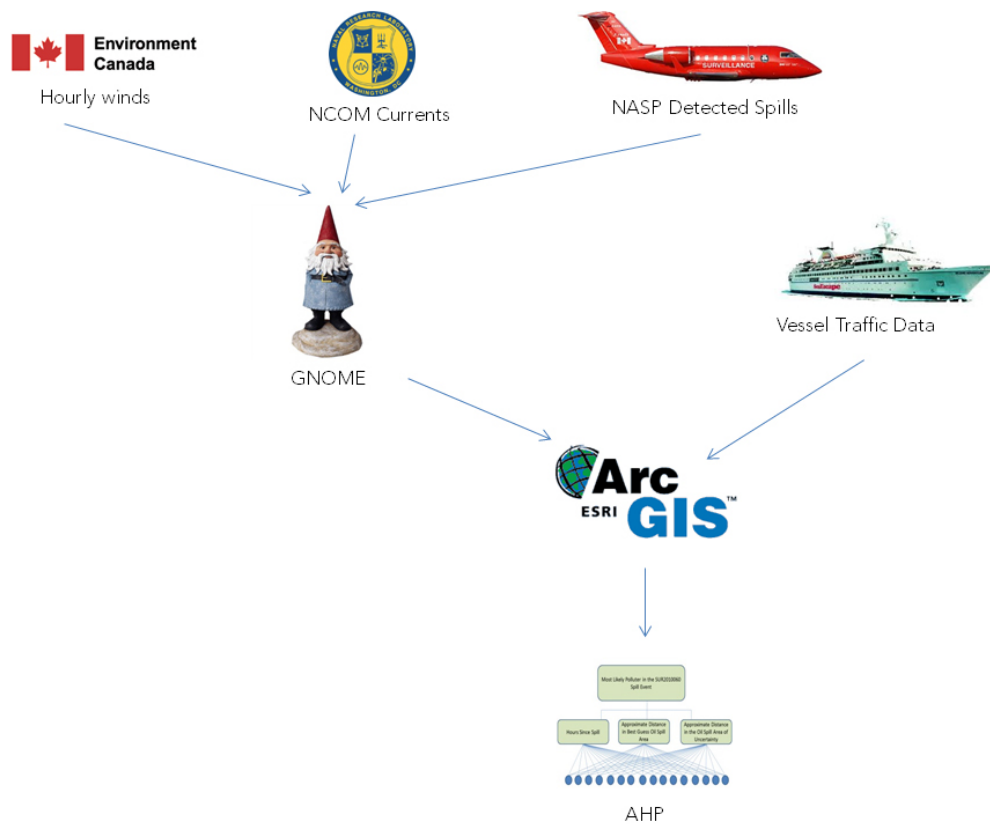


Figure 10. Elements of data and tools used in this thesis

AHP utilizes pairwise comparison to judge which of each pair of options is preferred. In AHP, a respondent is asked to make all pairwise comparisons so that a priority ranking can be made on a ratio scale for each objective.

Both the criteria and the vessels that are potentially responsible for an oil spill under each criteria, are compared against one another in terms of their importance in achieving the overall goal. For all criteria and the vessels under each criterion, a pairwise comparison reciprocal matrix (A) of judgments was made:

$$A = a_{ij} = \begin{pmatrix} 1 & a_1/a_2 & \dots & a_1/a_n \\ a_2/a_1 & 1 & \dots & a_2/a_n \\ \cdot & \cdot & 1 & \cdot \\ a_n/a_1 & a_n/a_2 & \dots & 1 \end{pmatrix} \quad (3)$$

Where a_i is the relative numerical preference between pairs of factors (from -9 to 9, as explained in Table 4) of the performance indicator i .

Table 4. Saaty's Scale of Importance (Saaty 1990)

Intensity of Importance	Definition	Explanation
1	Equal Importance	Two factors contribute equally to the objective
3	Moderately more important	Experience and judgment slightly favour one over the other.
5	Much more important	Experience and judgment strongly favour one over the other.
7	Very much more important	Experience and judgement strongly favour one over the other
9	Absolutely more important	The evidence favouring one over the other is of the highest possible validity

2,4,6,8	Intermediate Values	When compromise is needed
---------	---------------------	---------------------------

Relative priorities were derived for each of the potential culprit vessels from a comparison reciprocal matrix by solving:

$$\sum_{j=1}^n a_{ij}w_j = \lambda_{max} \quad \forall_i (a_{ji} = \frac{1}{a_{ij}} \text{ and } a_{ij} > 0) \quad (4)$$

where a is an individual element of the preference matrix, i and j indicate the i^{th} and j^{th} indicators, λ_{max} is the largest eigenvalue, and the weights (w) are normalized appropriately:

$$\sum_{i=1}^n w_i = 1 \quad (5)$$

The positive reciprocal matrix (A) and the set of equations (4) are then solved using the eigenvector method (described in section 5.1 and in appendix 2). The solution is normalized, as shown in equation (5). The consistency of this scoring used in the pairwise comparison is determined by using a consistency index (CI):

$$CI = \frac{\lambda_{max} - n}{n-1} \quad (6)$$

where n is the number of elements, or the dimension of the symmetrical matrix A . The matrix A is thus considered consistent with $w_i = a_{ij}w_j$ where its principal eigenvalue λ_{max} is equal to n . The matrix A is said to be inconsistent when $\lambda_{max} > n$. The variance of the error in estimating a_{ij} is then found as the consistency index (Saaty 1990). Furthermore, the consistency index can be compared to an average consistency index known as the random index (RI) to determine a consistency ratio:

$$CR = \frac{CI}{RI} \quad (7)$$

Table 5. Saaty's RI Values (Saaty 1998)

1	2	3	4	5	6	7	8	9	10	11	12	13	14	15
0.00	0.00	0.58	0.90	1.12	1.24	1.32	1.41	1.45	1.49	1.51	1.48	1.56	1.57	1.59

Perfect consistency occurs when $\lambda_{\max} = n$ (CR = 0); thus the closer λ_{\max} is to n , the better the consistency. CR values less than 10% are desired; but authors have accepted values up to 20% (Himes, 2007).

Chapter 5 Results and Discussion

This section presents the analysis of each spill event detected on the west coast by NASP over the course of 2010. The SUR2010060 spill event is used to illustrate the analysis procedure in detail, including worked out examples of eigenvector calculations using AHP. The results from AHP are discussed and probable polluters are determined for these spill events.

5.1 The SUR 2010060 Spill Event

The SUR2010060 spill event occurred on the Alaskan Marine Highway, where there were 16 vessels identified to have potentially passed through the bounding polygon of the spill event, as seen in Figure 11. In Table 6, the 16 vessels/alternatives are presented against the three 3 criteria (Hours since spill, Distance in the *Best Guess Area*, and Distance in the *Area of Uncertainty*).

Table 6. Potential Marine Polluters with Criteria Values in the SUR2010060 Spill Event

	Vessels	Hours Since Spill	Distance in <i>Best Guess</i> (Nautical Miles)	Distance in <i>Uncertainty</i> (Nautical Miles)
1	BRITTANY	7	0.00	0.70
2	COASTAL SEA	13	2.13	3.28
3	COMMODORE	32	2.83	2.83
4	EASTERN WIND	35	1.87	0.00
5	FROSTI	33	0.75	2.86
6	ISLAND BRAVE	36	0.72	0.00
7	ISLAND FURY	58	1.55	0.00
8	ISLAND NAVIGATOR	8	1.00	0.00
9	ISLAND SPIRIT	36	1.63	2.00
10	MUSKRAT	24	2.95	2.02
11	OCEAN CLIPPER	56	2.20	0.00

12	OCEAN KING	22	1.32	2.44
13	PACIFIC EAGLE	20	0.00	2.57
14	POLAR VIKING	18	2.77	1.49
15	PRIBILOF	13	2.18	3.17
16	WESTRAC II	13	2.20	3.13

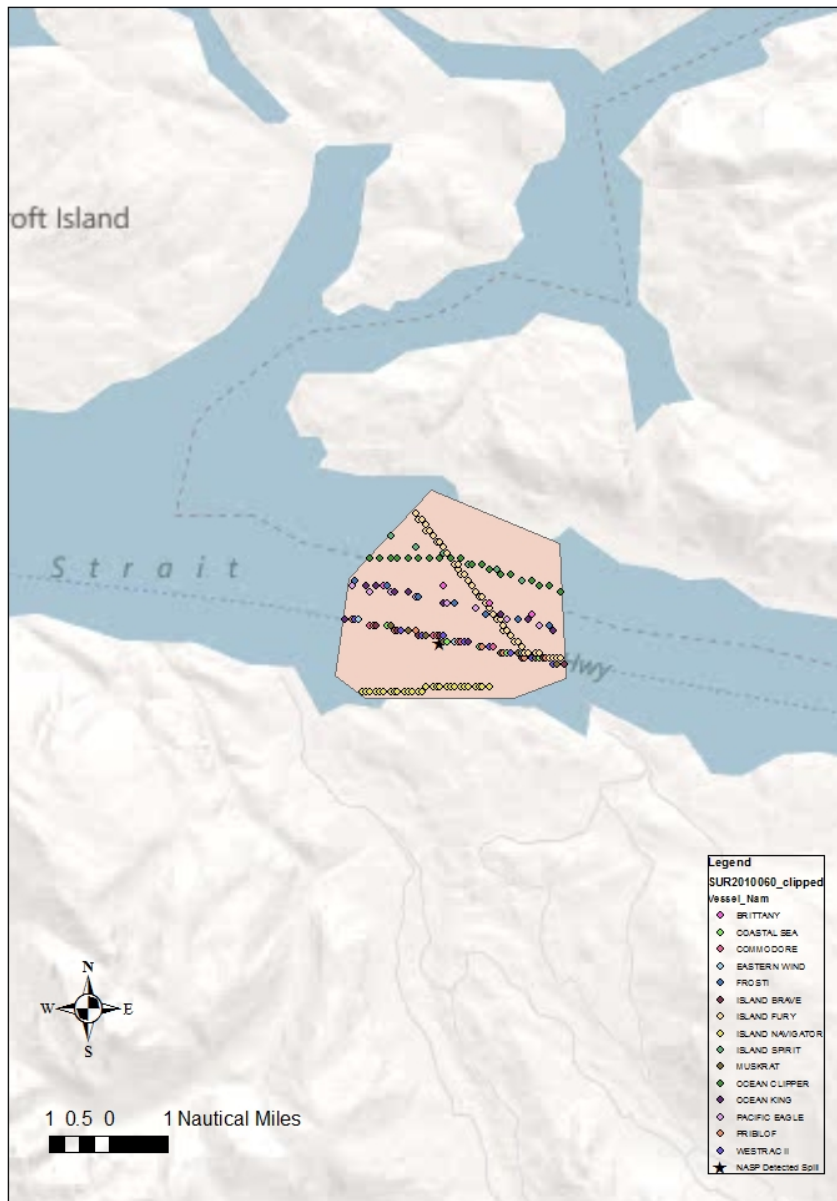


Figure 11. Vessels found within the SUR2010060 Spill Event Bounding Polygon

The structure of the AHP is shown in Figure 12.

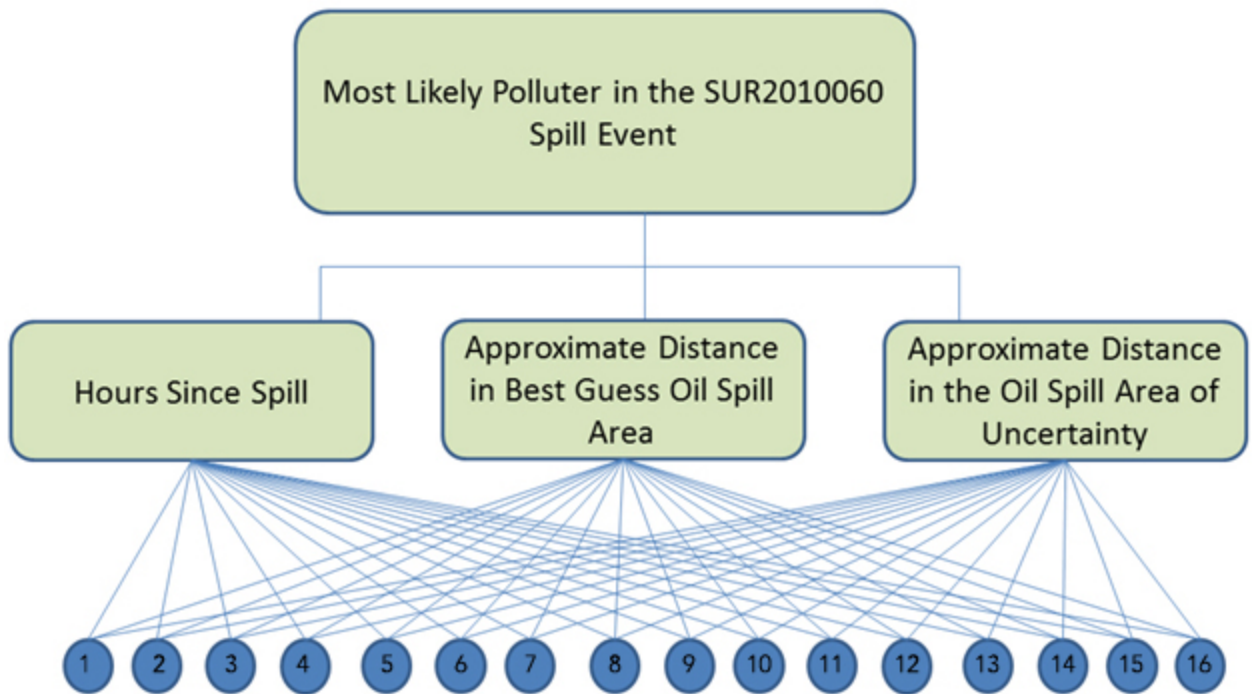


Figure 12. The structure of the SUR2010060 AHP (where the bottom 16 nodes represent the various ships)

With the structure defined, the pairwise analysis of the criteria and the vessels are performed.

First, the criteria are compared in a pairwise fashion as follows:

	<i>time (hrs)</i>	<i>best guess</i> (Nautical miles, Nm)	<i>uncertainty</i> (Nm)
<i>time (hrs)</i>	1.00	5.00	6.00
<i>best guess (Nm)</i>	0.20	1.00	3.00
<i>uncertainty (Nm)</i>	0.17	0.33	1.00

In the SUR2010060 case, it was deemed that in such a small geographic area, the time since the spill would be a heavily weighted criterion. The *best guess* and *uncertainty* areas largely overlap, especially during the first 24 hours of this spill, thus *hours* is ranked

fairly strong in comparison to the other two criteria. Secondly, based on the opinion of the author, the *best guess* area is more important than the area of *uncertainty*, from pairwise matrix above, as it describes the most likely area of origin for the oil spill. In this event, the area of *uncertainty* often overlaps with the area of *best guess* and provides a conservative estimate of where else the oil spill could have likely come from.

The eigenvector of the above matrix is then determined in three steps. First the pairwise matrix is raised to powers that are successively squared each time. Row sums are then calculated and normalized. When the difference between the sums in two consecutive calculations are the same after four decimal places, this value is the eigenvector (detailed example in appendix 2). The eigenvector was found to be (0.7172, 0.1947, 0.0881). The next stage is to calculate the largest eigenvalue, λ_{\max} , to then determine the consistency index for this analysis.

This is done by first multiplying the row of the matrix of judgments by the eigenvector, obtaining a new vector. The calculation for the first row is as follows:

$$1 \cdot 0.7172 + 5 \cdot 0.1947 + 6 \cdot 0.0881 = 2.2191$$

In similar fashion, the second and third row were calculated to be 0.6024 and 0.2725. These values represent the Aw and the AHP theory states that $Aw = \lambda_{\max}w$, so we can now get three estimates for λ_{\max} by dividing each element (2.2191, 0.6024, 0.2725) by the corresponding eigenvector element. This gives $2.2191/0.7172 = 3.094$, which is also the same value when applied to the rest of the eigenvector (0.1947 and 0.0881). Thus λ_{\max} is 3.094 and since this value is greater than n , the dimension of the matrix (3), then this is a valid number. The consistency index is calculated according to equation (6) as follows:

$$CI = \frac{\lambda_{\max} - n}{n - 1} = \frac{3.094 - 3}{3 - 1} = 0.047$$

Then using the RI values from literature (Table3), we determine the consistency ratio (CR)

$$CR = \frac{CI}{RI} = \frac{0.047}{0.58} = 0.08$$

This value is under the threshold $CR < 10\%$, thus the use of these eigenvectors to complete the final analysis is valid.

This process is now repeated for each of the ships according to each criterion. These three – 16x16 matrices are created to compare all the ships for time difference, distance travelled in the *best guess* area, and distance travelled in the area of *uncertainty*.

For the ‘time since spill’ criteria, values are first grouped into nine categories. Since the drifting of oil was done up to a 72 hour extent, the hours were partitioned on an 8 hour basis. For the vessels “Brittany” and “Island Navigator” that were found to have traversed the Alaskan Marine Highway 7 and 8 hours respectively prior to the spill being detected, they fit into the first time category. Vessels such as the “Ocean King” which was found to have traversed the Marine Highway 22 hours prior to the spill, was placed in category 3 (16-24 hours prior to the spill). Table 7 provides the 16 vessels’ categorizations according to the time window.

Table 7. Categorization of vessels based on time travelled prior to spill detection

Vessel Name	Time traveled prior to Spill Detection (hrs)	Category
BRITTANY	7	1
COASTAL SEA	13	2
COMMODORE	32	4
EASTERN WIND	35	4
FROSTI	33	4
ISLAND BRAVE	36	4
ISLAND FURY	58	7
ISLAND NAVIGATOR	8	1
ISLAND SPIRIT	36	4

MUSKRAT	24	3
OCEAN CLIPPER	56	7
OCEAN KING	22	3
PACIFIC EAGLE	20	2
POLAR VIKING	18	3
PRIBILOF	13	2
WESTRAC II	13	2

Based on this categorization, priorities were established. For example, the Island Fury is in category 7 compared to the Brittany which category 1. Since category 1 has a much greater weight than category 7 and because it is 6 categories away, the Island Fury would be assigned a score of $1/7$ compared to the Brittany, and the reciprocal score of 7 would be given to the Brittany compared to the Island Fury. Once this has been done for each vessel, the 16 x 16 matrix is created as shown in Table 8.

Table 8. The Pairwise Comparison of vessels based on hours prior to spill detection

	BRITTANY	COASTAL SEA	COMM.	EASTERN WIND	FROSTI	ISLAND BRAVE	ISLAND FURY	ISLAND NAV.	ISLAND SPIRIT	MUSKRAT	OCEAN CLIPPER	OCEAN KING	PACIFIC EAGLE	POLAR VIKING	PRIBILOF	WESTRAC II
BRITTANY	1.00	2.00	4.00	5.00	5.00	5.00	7.00	1.00	5.00	3.00	7.00	3.00	3.00	3.00	2.00	2.00
COASTAL SEA	0.50	1.00	3.00	3.00	3.00	3.00	6.00	0.50	3.00	2.00	6.00	2.00	2.00	2.00	1.00	1.00
COMMODORE EASTERN WIND	0.25	0.33	1.00	2.00	2.00	2.00	4.00	0.25	2.00	0.50	4.00	0.50	0.50	0.50	0.33	0.33
FROSTI	0.20	0.33	0.50	1.00	1.00	1.00	2.00	0.20	1.00	0.33	3.00	0.33	0.33	0.33	0.25	0.25
ISLAND BRAVE	0.20	0.33	0.50	1.00	1.00	1.00	2.00	0.20	1.00	0.33	3.00	0.33	0.33	0.33	0.25	0.25
ISLAND FURY	0.14	0.17	0.25	0.50	0.50	0.50	1.00	0.14	0.33	0.20	1.00	0.20	0.20	0.20	0.17	0.17
ISLAND NAVIGATOR	1.00	2.00	4.00	5.00	5.00	5.00	7.00	1.00	5.00	3.00	7.00	3.00	3.00	3.00	2.00	2.00
ISLAND SPIRIT	0.20	0.33	0.50	1.00	1.00	1.00	3.00	0.20	1.00	0.33	3.00	0.33	0.33	0.33	0.25	0.25
MUSKRAT	0.33	0.50	2.00	3.00	3.00	3.03	5.00	0.33	3.03	1.00	5.00	1.00	1.00	1.00	0.50	0.50
OCEAN CLIPPER	0.14	0.17	0.25	0.33	0.33	0.33	1.00	0.14	0.33	0.20	1.00	0.20	0.20	0.20	0.17	0.17
OCEAN KING	0.33	0.50	2.00	3.00	3.00	3.03	5.00	0.33	3.03	1.00	5.00	1.00	1.00	1.00	0.50	0.50
PACIFIC EAGLE	0.33	0.50	2.00	3.00	3.00	3.03	5.00	0.33	3.03	1.00	5.00	1.00	1.00	1.00	0.50	0.50
POLAR VIKING	0.33	0.50	2.00	3.00	3.00	3.03	5.00	0.33	3.03	1.00	5.00	1.00	1.00	1.00	0.50	0.50
PRIBILOF	0.50	1.00	3.00	4.00	4.00	4.00	6.00	0.50	4.00	2.00	6.00	2.00	2.00	2.00	1.00	1.00
WESTRAC II	0.50	1.00	3.00	4.00	4.00	4.00	6.00	0.50	4.00	2.00	6.00	2.00	2.00	2.00	1.00	1.00

Thus with the matrix defined, to evaluate these relative ratings a similar process to that which was applied to the criteria is followed. The eigenvectors were determined to be (0.0150, 0.0815, 0.1289, 0.05, 0.021, 0.021, 0.05, 0.0308, 0.05, 0.1289, 0.0815, 0.0331, 0.0147, 0.1309, 0.0815, 0.0815). The consistency index and consistency ratio were 0.0203 and 0.01277 respectively, which show that the prioritization scheme is valid.

The same method is applied for both the distance in the *best guess* and distance in the area of *uncertainty* criteria. The categorization schemes assumed distance intervals of 0.5 nautical miles, which is reasonable given that vessels were seen to travel distances of up to 3.28nm in the area of uncertainty.

Table 9. Classification of vessels for distances in the area of *best guess* and *uncertainty*

Vessels	Distance in Best Guess (Nautical Miles)	Classification for Distance in Best Guess	Distance in Uncertainty (Nautical Miles)	Classification for Distance in Area of Uncertainty
BRITTANY	0.00	1	0.70	2
COASTAL SEA	2.13	5	3.28	7
COMMODORE	2.83	6	2.83	6
EASTERN WIND	1.87	4	0.00	1
FROSTI	0.75	2	2.86	6
ISLAND BRAVE	0.72	2	0.00	1
ISLAND FURY	1.55	4	0.00	1
ISLAND NAVIGATOR	1.00	3	0.00	1
ISLAND SPIRIT	1.63	4	2.00	5
MUSKRAT	2.95	6	2.02	5
OCEAN CLIPPER	2.20	5	0.00	1
OCEAN KING	1.32	3	2.44	5
PACIFIC EAGLE	0.00	1	2.57	6

POLAR VIKING	2.77	6	1.49	3
PRIBILOF	2.18	5	3.17	7
WESTRAC II	2.20	5	3.13	7

By producing two – 16 x 16 matrices for both of these sets of criteria, Table 10 shows the respective eigenvectors.

Table 10. Eigenvectors for distances in the area of *best guess* and *uncertainty*

Vessels	Distance in Best Guess	Distance in Uncertainty
BRITTANY	0.0150	0.0207
COASTAL SEA	0.0815	0.1393
COMMODORE	0.1289	0.0918
EASTERN WIND	0.0500	0.0174
FROSTI	0.0210	0.0880
ISLAND BRAVE	0.0210	0.0143
ISLAND FURY	0.0500	0.0143
ISLAND NAVIGATOR	0.0308	0.0143
ISLAND SPIRIT	0.0500	0.0607
MUSKRAT	0.1289	0.0607
OCEAN CLIPPER	0.0815	0.0143
OCEAN KING	0.0331	0.0620
PACIFIC EAGLE	0.0147	0.0918
POLAR VIKING	0.1309	0.0319
PRIBILOF	0.0815	0.1393
WESTRAC II	0.0815	0.1393

The values for the consistency index are 0.0203 and 0.0414, which lead to consistency ratios of 0.0127 and 0.0260 for the distance in the *best guess* and *distance in the area of uncertainty*, respectively. Since these values were under the threshold of CR < 10%, it was deemed that these values were valid for application.

With the sets of eigenvectors calculated for the criteria matrix and each of the respective ships for each of the above mentioned criteria, the multiplication of the 16 x 3

eigenvectors of the prioritized vessel-to-criteria matrix (respective eigenvectors of the 16 x 16 matrices described above) by the 3 x 1 eigenvectors of the prioritized criteria was made to determine the ranking of the vessels. Table 11 shows the rankings of each of the vessels.

Table 11. Vessel Rankings in the SUR2010060 Spill Event

Vessels	Overall Score
BRITTANY	0.1176
COASTAL SEA	0.0995
COMMODORE	0.0716
EASTERN WIND	0.0414
FROSTI	0.0348
ISLAND BRAVE	0.0251
ISLAND FURY	0.0251
ISLAND NAVIGATOR	0.0790
ISLAND SPIRIT	0.0300
MUSKRAT	0.1091
OCEAN CLIPPER	0.0343
OCEAN KING	0.0609
PACIFIC EAGLE	0.0257
POLAR VIKING	0.0773
PRIBILOF	0.0833
WESTRAC II	0.0854

Thus the Brittany is ranked first, the Muskrat is ranked second and the Coastal Sea is ranked third. These three options have good face validity, as 'Brittany' was the first vessel to have traversed the Alaskan Marine Highway and to have gone directly through the spill area prior to detection of the spill. The Brittany is a fishing vessel from the United States built in the late 1970s. Due to the greater emphasis on the weighting of the time aspect in the AHP analysis, the Brittany was chosen as the most likely polluter.

'Muskrat', another fishing vessel from the United States was a close second as it traversed directly through the area of *best guess* and *uncertainty*. 'Coastal Sea' was also a top priority vessel as it traversed extensively in both areas in a short amount of time after the spill incident. It was also a plausible candidate as it is an American General Cargo vessel built in the 1950s.

5.2 The SUR2010044 Spill Event

This spill was detected within the Alberni Inlet, south of Port Alberni on June 23. The volume of this spill was approximately 13.2 L. From a three-day run in GNOME, it was found that the spill could have occurred 72 hours prior to its detection, however after 30 hours of simulation time a majority of the splots (70%) had been beached, so it is believed that the spill most likely occurred within 30 hours prior to detection from the southern direction. Thus the bounding polygon was created which spanned 6.32 nautical miles in the north-south direction over the entire width of the inlet which spanned from 1.5 – 2 nm in the east-west direction. Figure 13 shows the vessels' tracks clipped within this bounding polygon.

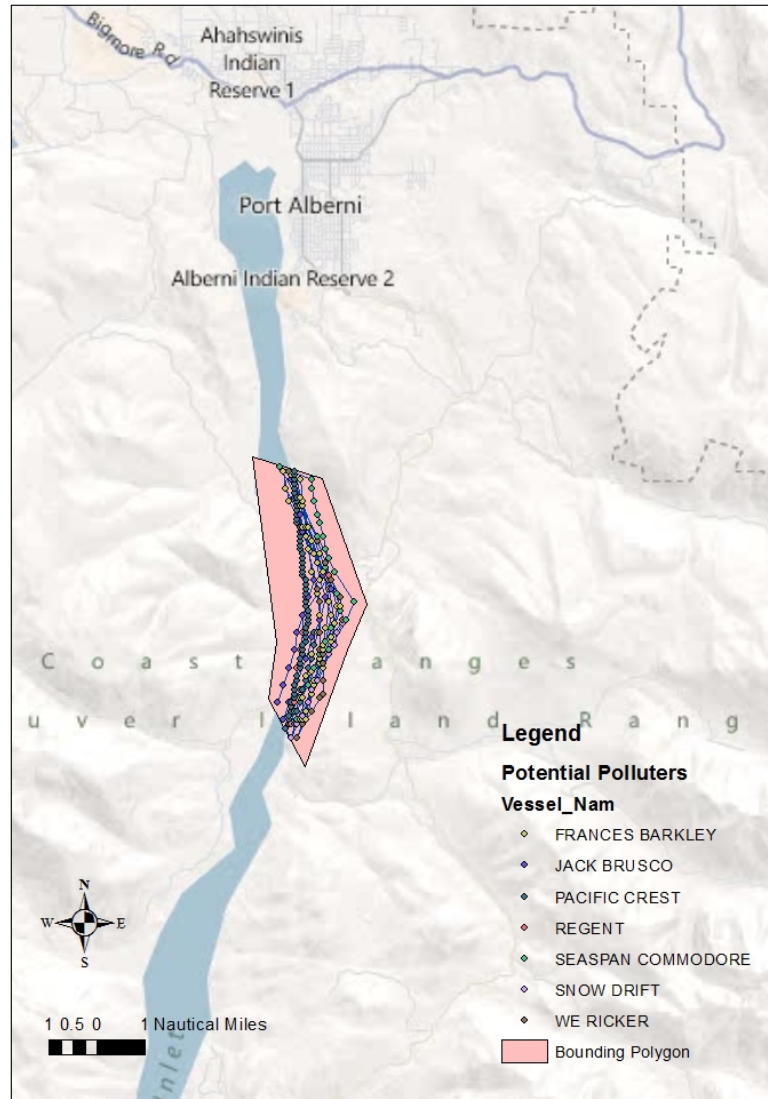


Figure 13. Potential Polluters in the SUR2010044 Spill

From Figure 13, we see that there are 7 vessels that went through the area of the spill. These vessels reported at least 12 positions each during this time, thus they offered an adequate number of vessel positions for analysis. Among the position sources, manual positioning and dead reckoning positioning were found. What makes this scenario

interesting is that some vessels suspected of polluting tend to make multiple trips through the area of the spill. So while we have 7 different vessels, there are 16 individual trips. Of these 7 different vessels, it was found that only 3 vessels, over the course of 4 trips had passed through either the area of best guess or area of uncertainty of this spill. These trips and vessels are listed in Table 12.

Table 12. Potential Polluters from the SUR2010044 Spill Event

	Vessel Name	Hours prior to spill detection	Distance in Best Guess	Distance in Uncertainty	Vessel Type
1	FRANCES BARKLEY (1)	12	0.35	0.31	Canadian Passenger/Vehicle Vessel
2	FRANCES BARKLEY (2)	3	0.22	0.26	Canadian Passenger/Vehicle Vessel
3	JACK BRUSCO	28	0	1.17	Tug (United States)
4	PACIFIC CREST	22	0.44	1.41	Tug (Australian)

In this spill, the structure of the AHP is seen in Figure 14.

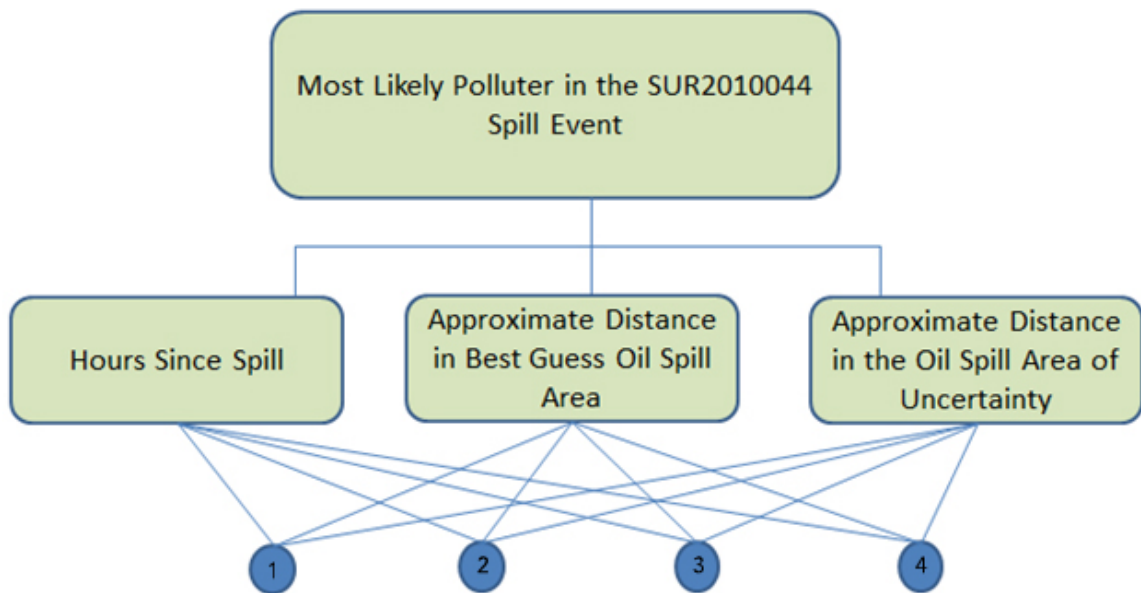


Figure 14. The structure of the SUR2010044 Spill Event AHP (where the nodes represent each transit)

The criteria pairwise comparison matrix is the same as that from the SUR2010060 Spill Event.

	time (hrs)	best guess (Nm)	uncertainty (Nm)
time (hrs)	1.00	5.00	6.00
best guess (Nm)	0.20	1.00	3.00
uncertainty (Nm)	0.17	0.33	1.00

Thus, the eigenvector is identical to that from the SUR2010060 spill event, (0.7172, 0.1947, 0.0881), and the CR is 0.081 which shows consistency in this approach.

For the time that a vessel traveled past the area of the spill prior to detection, similar time windows of 8 hours were applied. Table 13 shows the ranking of the 4 vessels.

Table 13. Categorization of the possible polluters in the SUR2010044 Spill Event by time traveled prior to spill detection

Vessel Name	Time traveled prior to Spill Detection (hrs)	Category
FRANCES BARKLEY (1)	12	2
FRANCES BARKLEY (2)	3	1
JACK BRUSCO	28	4
PACIFIC CREST	22	3

The respective matrix corresponding to Table 13 is shown in Table 14. The eigenvector was calculated as (0.2772, 0.4673, 0.954, 0.1601) with a CR of 0.018.

Table 14. The Pairwise Comparison Matrix based on Hours for the SUR2010044 Spill

Event

	FRANCES BARKLEY (1)	FRANCES BARKLEY (2)	JACK BRUSCO	PACIFIC CREST
FRANCES BARKLEY (1)	1.00	0.50	3.00	2.00
FRANCES BARKLEY (2)	2.00	1.00	4.00	3.00
JACK BRUSCO	0.33	0.25	1.00	0.50
PACIFIC CREST	0.50	0.33	2.00	1.00

For the classification of the *Best Guess* and *Uncertainty* areas of the spill, the thresholds of 0.1 and 0.2 nautical miles were used, respectively. Table 15 shows the classification of each alternative.

Table 15. Categorization of the possible polluters in the SUR2010044 Spill Event based on distance in the area of best guess and uncertainty

Vessels	Distance in Best Guess (Nautical Miles)	Classification for Distance in Best Guess	Distance in Uncertainty (Nautical Miles)	Classification for Distance in Area of Uncertainty
FRANCES BARKLEY (1)	0.35	4	0.31	2
FRANCES BARKLEY (2)	0.22	3	0.26	2
JACK BRUSCO	0	1	1.17	6
PACIFIC CREST	0.44	5	1.41	7

Following the same technique as for the time prior to detection criteria, with the end result yields eigenvectors of (0.2844, 0.1699, 0.0729, 0.4729) and (0.0751, 0.0751, 0.3329, 0.5168) and CR values of 0.029 and 0.019 for the *best guess* and *uncertainty areas*, respectively.

With all the eigenvectors computed, the rankings for each transit were made and the following results were found.

Table 16. Normalized results of the AHP process applied to the SUR2010044 Spill Event

Vessels	Normalized Results
FRANCES BARKLEY (2)	0.3749
FRANCES BARKLEY (1)	0.2608
PACIFIC CREST	0.2524
JACK BRUSCO	0.1120

Thus the two transits of the Frances Barkley are ranked the highest followed closely by the Pacific Crest and the Jack Brusco. These numerical values are acceptable, however further scrutiny of the vessels is necessary. The Frances Barkley, shown in figure 15, is a passenger vessel that transits these waters twice a day, every day.



Figure 15. The MV Frances Barkley

For over 60 years, it has served as the mail and freight service that has run day trips between Alberni and Barkley Sound. This makes this vessel an unlikely polluter, thus raising the probability of the culprit being the Pacific Crest or the Jack Brusco. These two are foreign flagged tugs. In such a case, perhaps these vessels were towing another leaky vessel/object, where it would be worthwhile to enquire whether the Frances Barkley's crew had noticed anything unusual about these two tugs.

5.2.1 Sensitivity Analysis on the AHP of the SUR2010044 Spill Event

The weighting of the criteria matrix currently favours the criteria of *time traveled prior to spill event*, over the distances spent in the area of *best guess* and *uncertainty*. These are in the expert opinion of the author and this section compares the weighting schemes by changing the weights of each criterion, while holding the others constant. For example, the criteria of time traveled prior to spill detection can be changed from one to nine, while the distance in the area of best guess and uncertainty are held at five and nine, respectively. This has been done for each criteria individually and the normalized rankings of all 4 potential culprits are shown in Figures 16, 17 and 18.

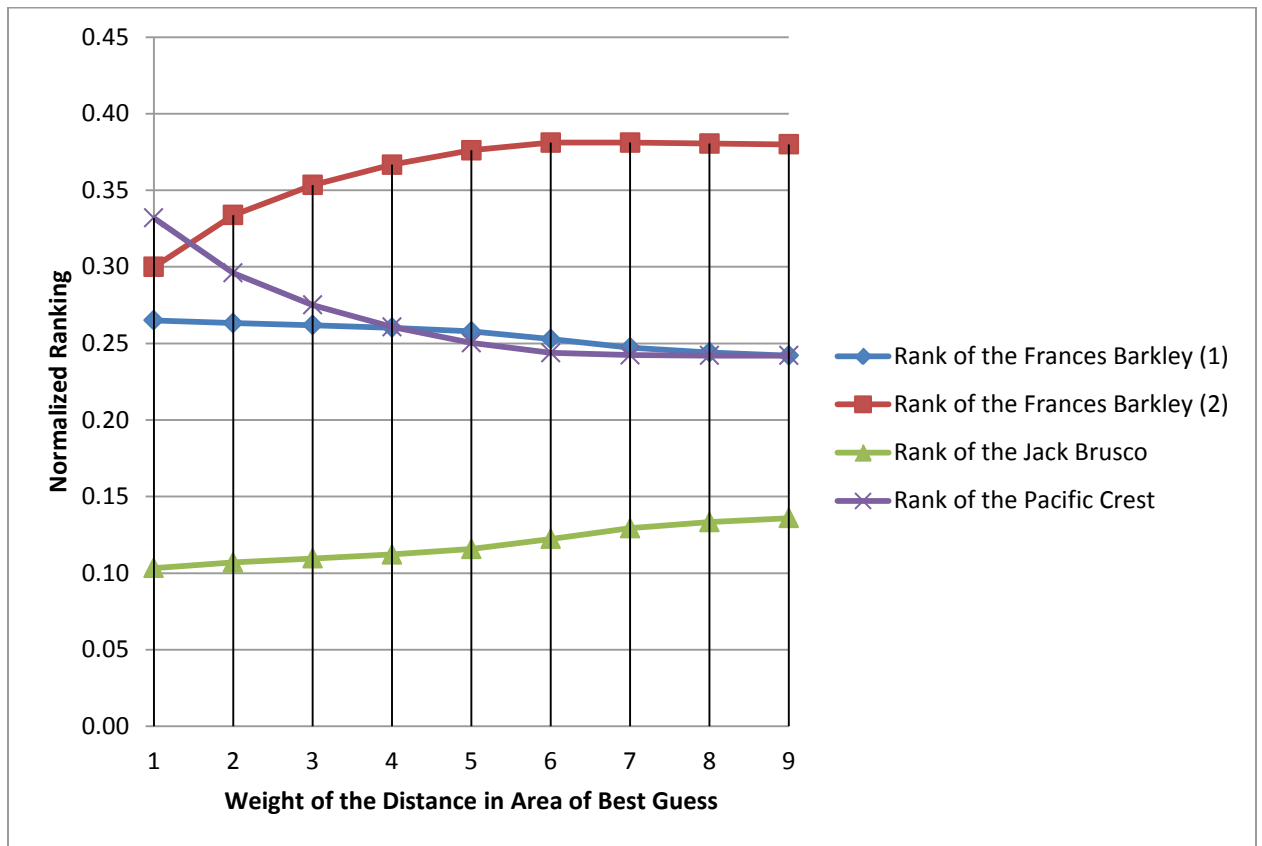


Figure 16. Normalized ranking of vessels as weight of the distance in area of *best guess* criteria varies from one to nine

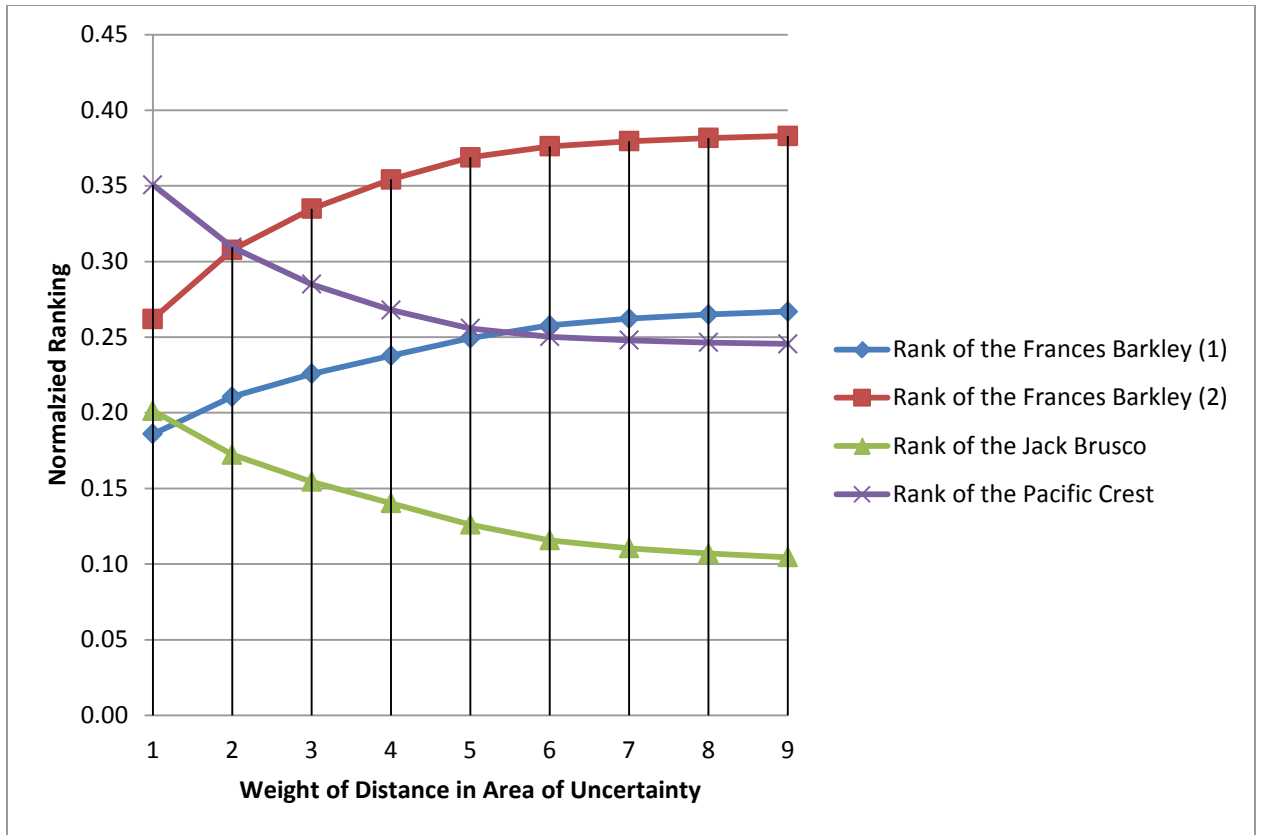


Figure 17. Normalized ranking of vessels as weight of the distance in area of *uncertainty* criteria varies from one to nine

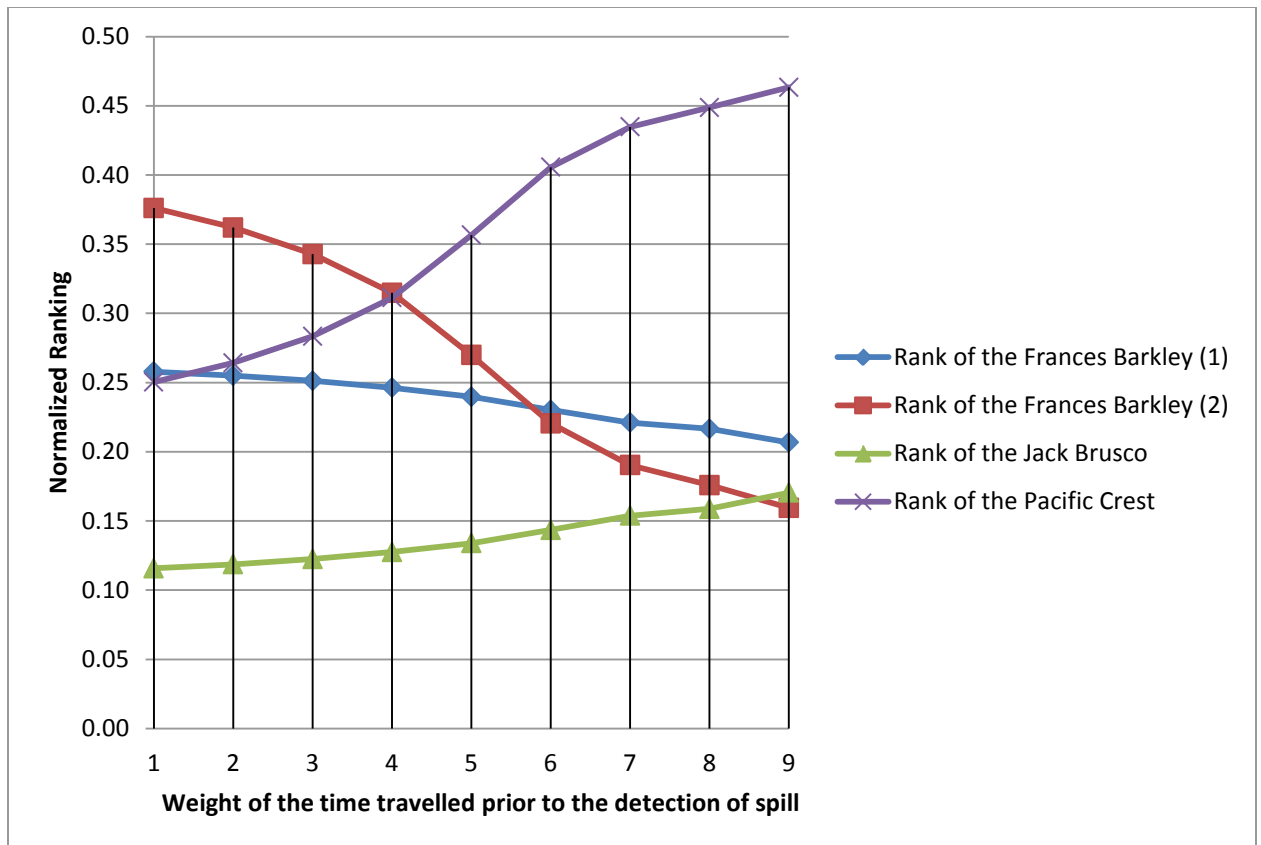


Figure 18. Normalized ranking of vessels as weight of *time* travelled prior to the detection of spill criteria varies from one to nine

This tests the sensitivity of the AHP to the different weightings of criteria. This is important, because different experts may weigh the criteria differently as there is no single objective value that applies.

When comparing the results from Figure 16 and 17, only in cases where those weights are equivalent to that of the time, are there significant changes to the results. In all the figures, the Pacific Crest is the only vessel that ranks higher than the Frances Barkley (2); it ranks higher when the weights for either of the distances are equivalent to the weight applied to the criterion of time traveled prior to spill detection. This is due to the fact that the Pacific Crest has the greatest distance in both the area of best guess and uncertainty, compared to all of the other possible culprits. From Figure 18, the changes

are much more sensitive to weight changes compared to Figure 16 and 17. Holding the time criteria consistently weighted at high importance precludes variations of the other weights to affect the rankings, unless those weights are equivalent to that of the time criteria. Conversely, by varying the weight of the time criteria, changes are much more dramatic, as its importance becomes equivalent to that the other criteria. Thus the ranking for this event is most sensitive when a single criterion that was previously dominant is made equivalent to that of the other pieces of criteria. This is interesting to note as different researchers may emphasize the distance travelled in certain areas to be of more importance than that of the time travelled prior to a spill.

Chapter 5.3: The SUR2010075 Spill Event

This particular spill was located on the Agamemnon Channel. The Agamemnon Channel is a strait located at the mouth of the Jervis Inlet on the South Coast which separates Nelson Island from the mainland of the Sunshine Coast. According to locals, this channel is used primarily by ferry traffic and local pleasure craft (Shangan Webservices, 2012). By modeling this spill in GNOME, it was determined that the origin of the spill would have come from within a 1 nautical mile distance in either the north or south direction within 45 hours of the time of detection (as approximately 80% of the spill would have been beached by that time). However this is one of the few spots that have little-to-no coverage by any vessel traffic monitoring systems, as seen in Figure 19, where the closest vessel position is over 10 nautical miles away from the location of the detected spill.

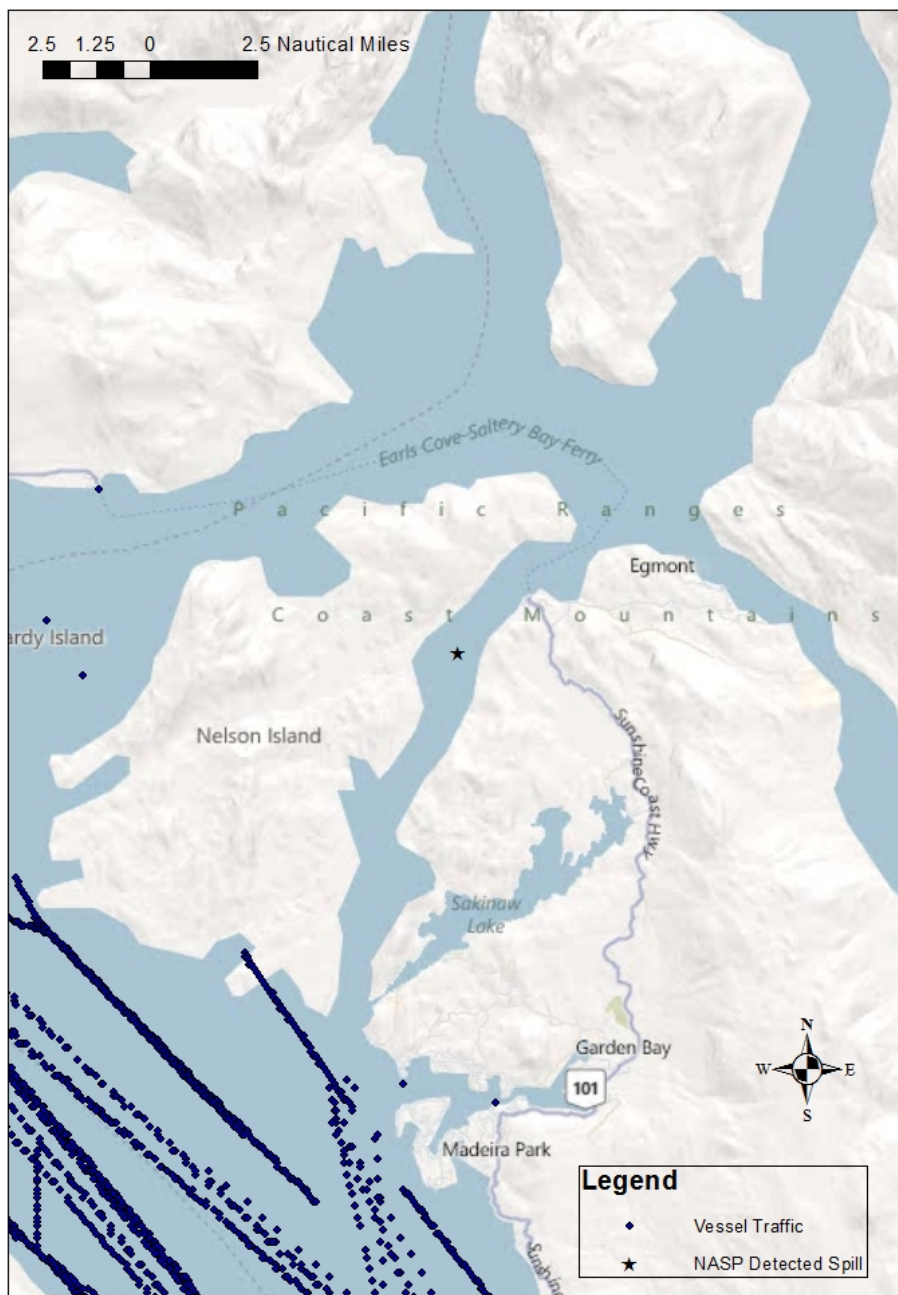


Figure 19. Vessel Traffic around the SUR2010075 Spill Event

Further analysis of historical detected spills (pre-2010), indicate that four spills were

recorded in this particular channel during the time span of 2008 – 2010. These spills are characterized in Table 17.

Table 17. Historic Oil Spills (2008 – 2010) in the Agamemnon Channel

Flight Number	Latitude	Longitude	Year	Month	Day	Time (UTC)	Volume (L)
SUR2008040	49.65700	-124.079	2008	3	22	2039	1.3
SUR2008079	49.76367	-124.000	2008	6	21	1924	0.01
SUR2008092	49.75683	-124.016	2008	7	31	1734	0.6
SUR2010075	49.73883	-124.037	2010	11	3	2106	2.11

From Table 17 and Figure 20 it appears that this area is fairly susceptible to spill incidents and should be monitored more in the future. Unfortunately, there is inadequate vessel traffic data to analyze this spill scenario at this time.

From future coverage plans for AIS, it is very possible that vessel positions in the vicinity of this spill and along the Agamemnon Channel will be captured by the Texada Island and the Bowen Island AIS towers. Approximate 40 nm coverage ranges are shown for both towers in relation to this spill in Figure 21.



Figure 20. Historic Oil Spills (2008 – 2010) in the Agamemnon Channel

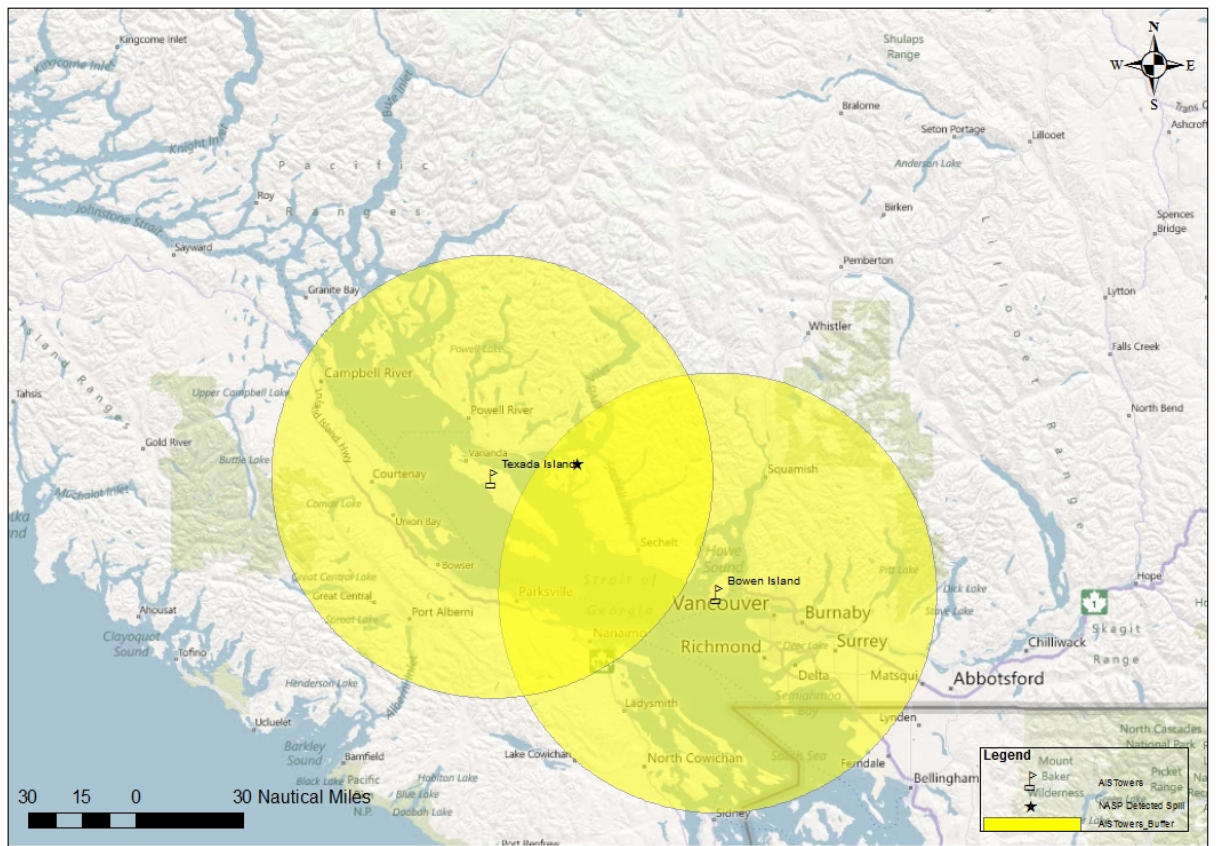


Figure 21. AIS Coverage from Texada Island and Bowen Island AIS Towers in relation to the SUR2010075 Spill Event

5.4 The SUR2010071 Spill Event

This particular spill that happened just north of Prince Rupert along the Hecate Strait was detected on October 28th at 21:49 UTC. This spill was one of the smaller incidents of the year (0.3 L) and the location is plotted in Figure 22, with an aerial picture provided in Figure 23.



Figure 22. The SUR2010071 Spill Event near Prince Rupert



Figure 23. Aerial shot of Prince Rupert that depicts the approximate spill area

This spill was modeled in GNOME, where it was found that under the conditions that existed prior to the detection of this small spill, it is likely that it occurred no more than 12 hours prior to detection. This is the case because 100% of the *best guess* splots were beached under a 9 hour backcast, and again when checked at 12 hours prior to detection. Figure 24 shows the chronological drift sequence (every 3 hours for this spill), illustrating that a majority of the splots were no longer in play after going back 9-12 hours prior to the detection of this spill.

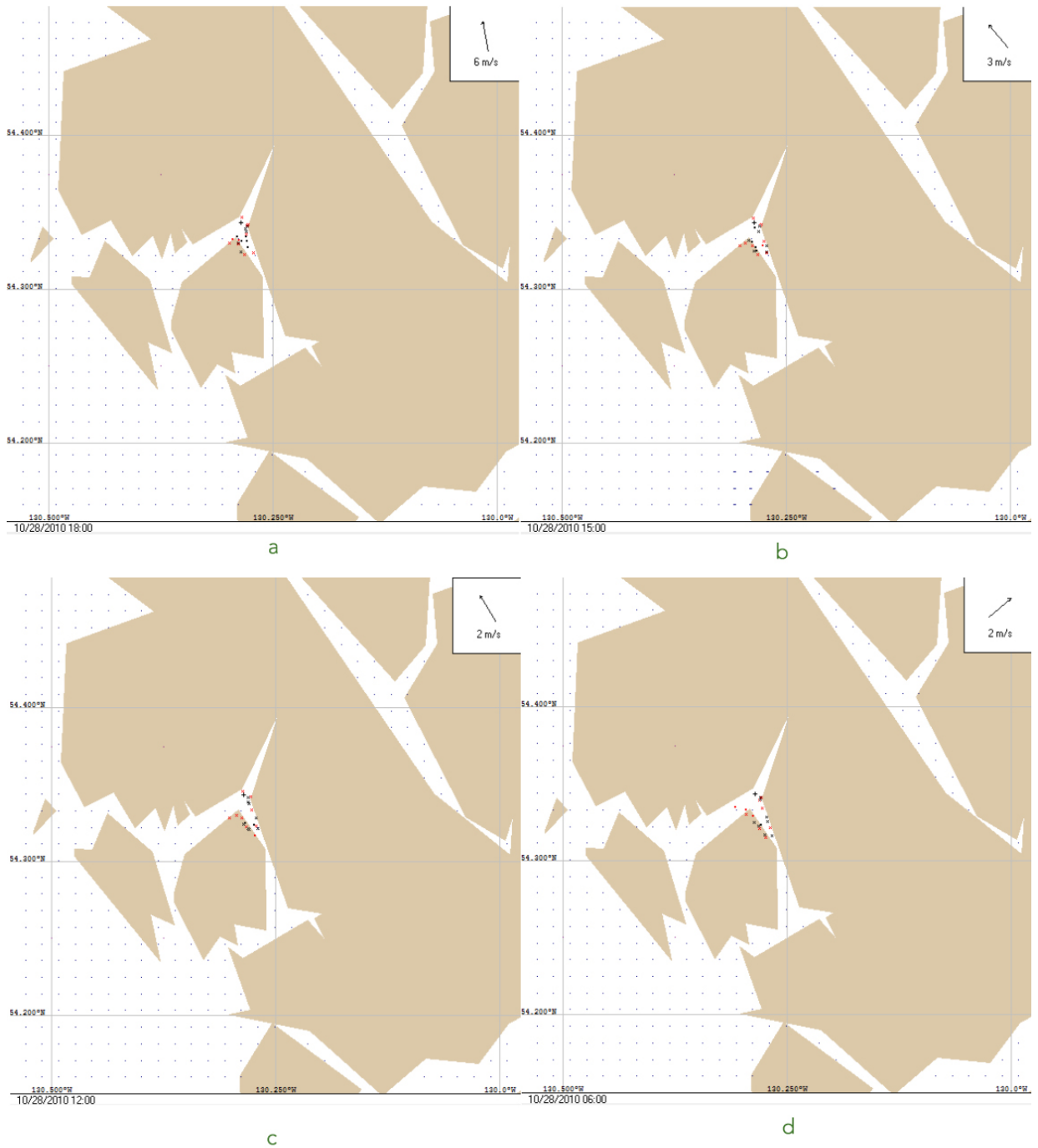


Figure 24. The chronological drift sequence of the SUR2010071 Spill Event at an interval of 3 hours, a – 3 hours prior to spill detection, b – 6 hours prior to spill detection, c – 9 hours prior to spill detection, d – 12 hours prior to spill detection

Thus a bounding polygon was made based on beached splots after 12 hours to at least determine all vessel traffic in the area. It was then found that there were 3 vessels that

traversed the area over the three-day period (Table 18).

Table 18. Vessels that passed by the SUR2010071 Spill Event Bounding Polygon

Vessel Name	# Reports	Hours Prior to Spill Detection	Vessel Type
Cadal (1)	4	43	Tug
Cadal (2)	7	58	Tug
Castle Lake (1)	48	61	Tug
Castle Lake (2)	19	42	Tug
Igenika (1)	11	64	Tug
Igenika (2)	12	43	Tug

However from these results, no vessel was actually found to have travelled the area around the time to the detection of this spill, thus it was unlikely that any of these vessels were the culprits for this spill. The closest tracked vessel traversed the area almost 43 hours prior to spill detection, which makes it a highly unlikely culprit. Due to the small size of this spill, it may very well have come from a non-reporting, small sized pleasure craft. In the future, AIS will be another source of data which may add context and help clarify the situation. Figure 25 shows the future approximate AIS coverage (40 nm) from the Mount Hayes AIS tower.

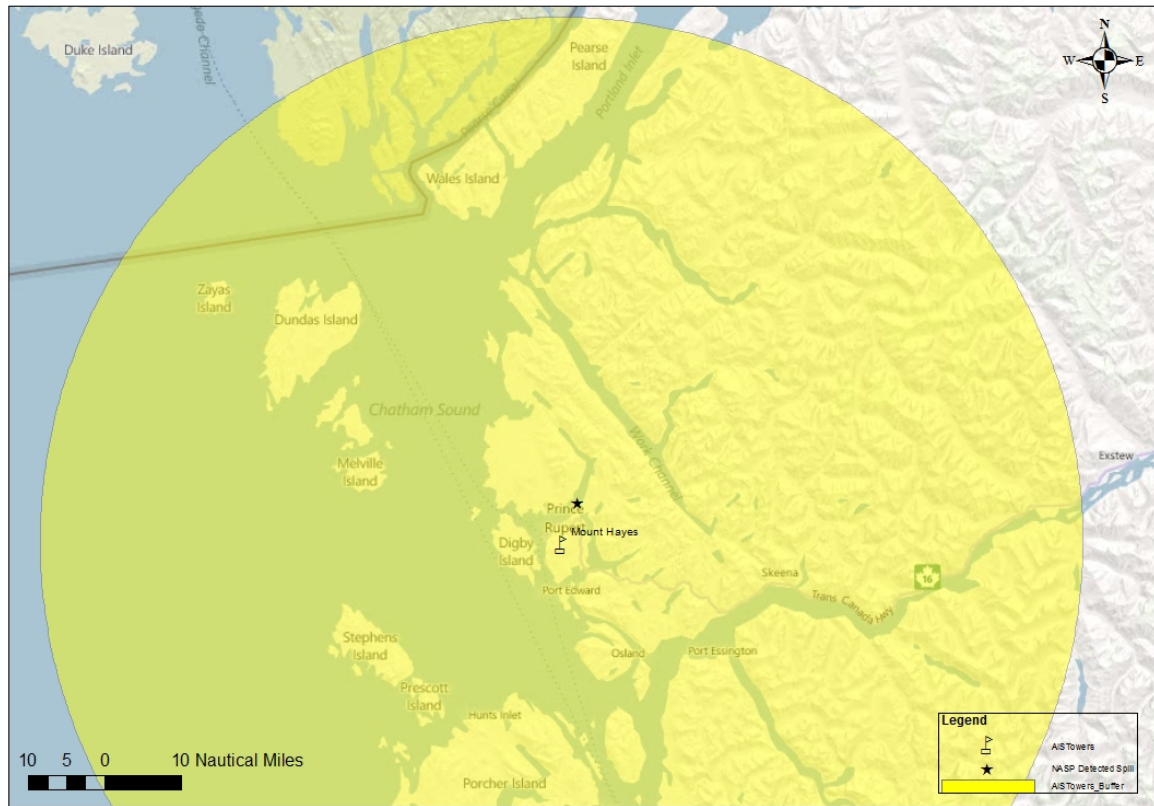


Figure 25. AIS Coverage from Mount Hayes AIS tower in relation to the SUR2010071 Spill Event

5.5 The SUR2010059 Spill Events

SUR2010059 represents 2 spill events that occurred near one another, 180 nautical miles offshore in the open ocean (Figure 26).



Figure 26. The SUR2010059 Spill Events

For the purpose of this analysis, each spill will be analyzed individually (SUR2010059_1 & SUR2010059_2) and then collated to see if the analyses point to a single polluter.

For SUR2010059_1, from the plots file it appears that the spill came from the southwestern direction. For SUR2010059_2, a pattern of drifting from the north was seen. While wind patterns used were identical, the currents at each spill, approximately 43 nautical miles apart, resulted in a different drifting pattern. Figure 27 shows the bounding polygon for each spill.

The VTOSS (Figure 27) and LRIT (Figure 28) traffic data sets were both analyzed. Since LRIT provided sparse temporal coverage, it did not prove to be helpful on an inshore basis. However, it proved to be very helpful at the offshore level. In comparing the two data sources, VTOSS showed 1 vessel in the areas of these 2 spills, while LRIT showed 11 different vessels to have gone through these areas. LRIT also accounted for the one relevant vessel that was captured with VTOSS. Thus LRIT was the only data source used for vessel traffic in the further analysis of these spills. The 11 vessels of interest are shown in Figure 29.

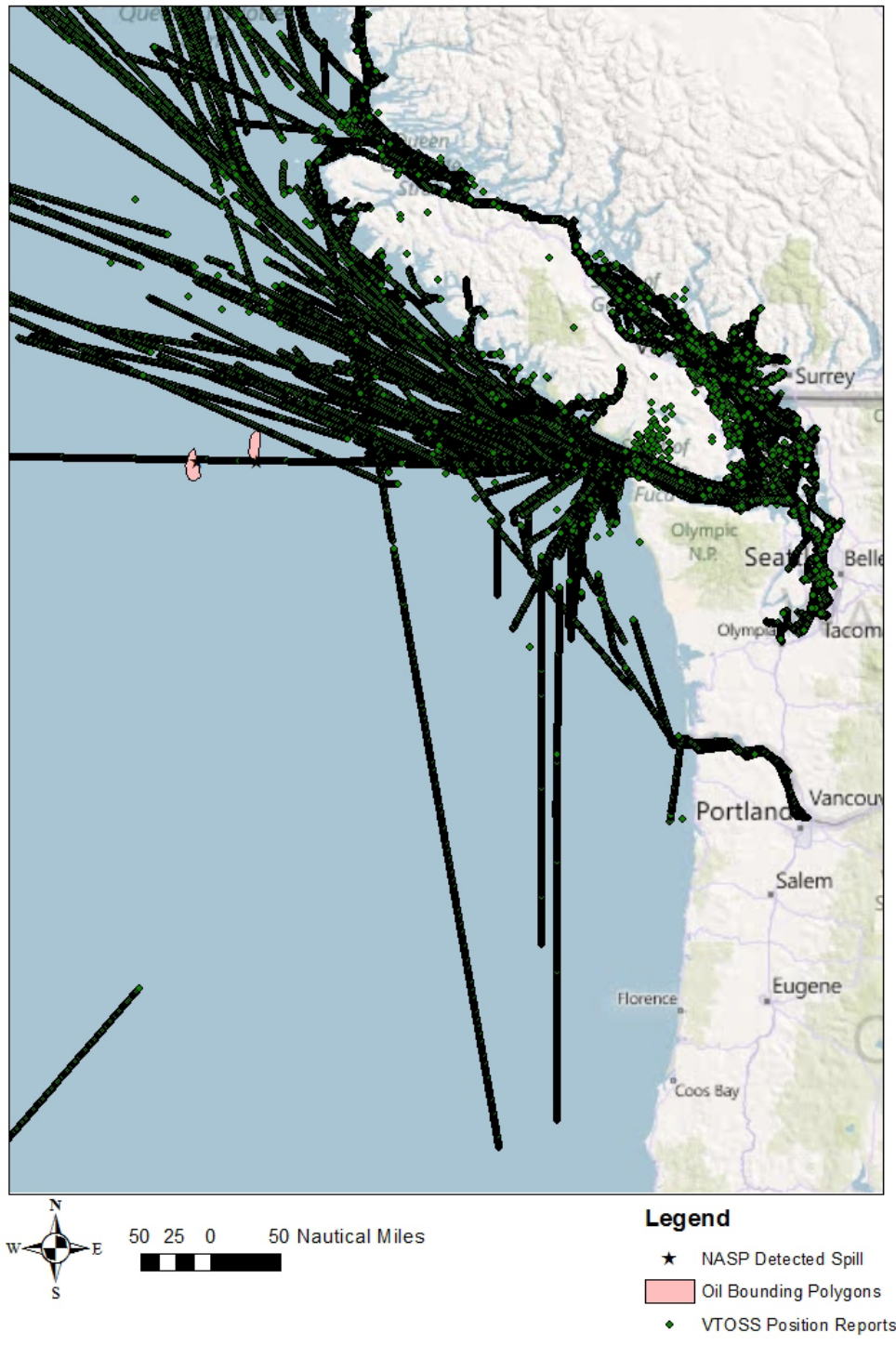


Figure 27. VTOSS Data around the SUR2010059 Spill Events

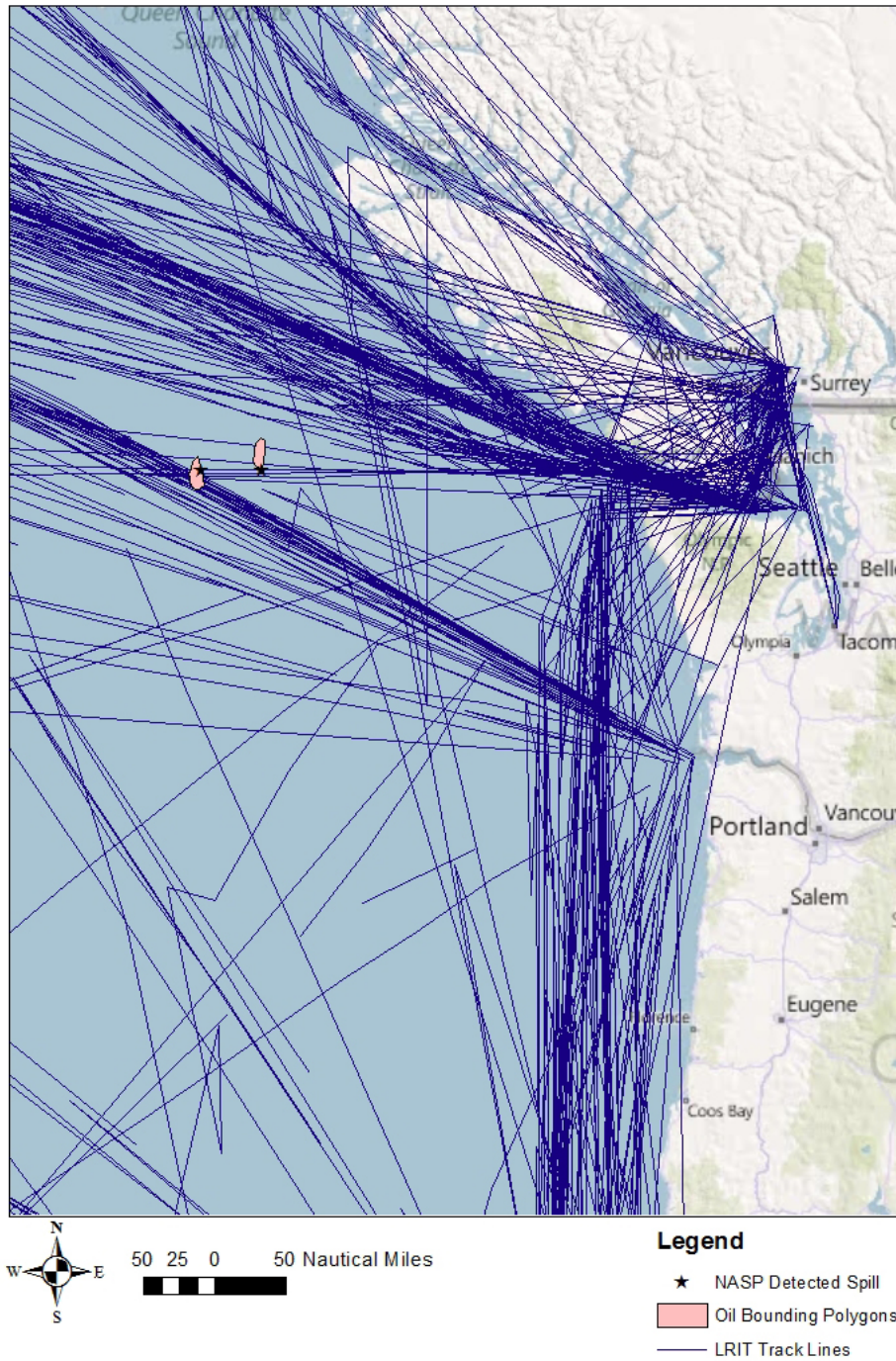


Figure 28. LRIT Traffic in and around the SUR2010059 Spill Event

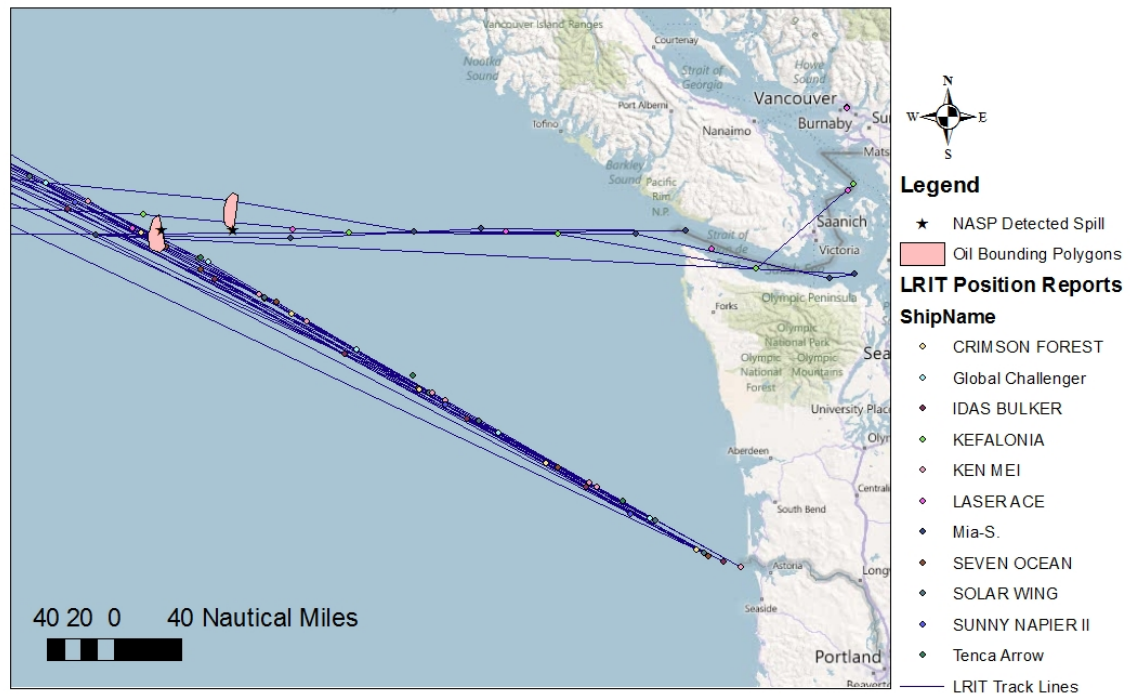


Figure 29. Potential Polluters in the SUR2010059 Oil Spill Areas

Since LRIT standard reports are at six-hour intervals, more processing is required than with VTOSS data, to calculate the intersection of a ship's path with the projected spill area. Table 19 lists the possible polluters for the spill incident SUR2010059_1.

Table 19. Possible polluters for the SUR2010059_1 Spill Incident

IMO	Name	Heading
8708244	SOLAR WING	Heading to US
9059119	SUNNY NAPIER II	Heading to US
9111369	IDAS BULKER	Leaving US
9122887	SEVEN OCEAN	Leaving US
9162411	GLOBAL CHALLENGER	Leaving US
9205847	KIND SEAS	Leaving US
9206140	CRIMSON FOREST	Leaving US
9310721	JASMINE ACE	Leaving US
9310745	ANSAC KATHRYN	Leaving US
9384863	LASER ACE	Heading to Canada

On the assumption that vessels travelled in a straight line between each pair of reporting points, the straight distances through the areas of *best guess*, and *uncertainty* were measured the same way as previous spills using VTOSS. The time to spill was determined by calculating the approximate nautical mile per minute speed of a vessel and dividing this value by the distance to the bounding polygon.

For example, for the 'Anzac Kathryn' that reported at exactly a 360 minute interval, the distance between the two position reports that straddled the bounding polygon of SUR2010059_1 was measured to be 107.74 nm. Thus its speed was approximately 0.299 nm per minute. By measuring the distance of its position closest to shore, to the point at which the line intersects with the bounding polygon of the SUR2010059_1 spill, this distance (64.8 nm) is divided by the speed (nm/minute) to find the approximate difference in time from the first chronological position report. By adding this difference, the approximate time at which the vessel would have passed through the area of the spill is determined and used as a metric to provide the local, hourly polygons for the *area of best guess* and *area of uncertainty*.

Among the possible polluters, the 'Laser Ace' was the only vessel headed to Canada

and the only possible polluter in the SUR2010059_2 spill event, while the other possible polluters were only applicable to the SUR2010059_1 spill and were either en route to or departing from the United States.

For the SUR2010059_2 spill, table 20 shows all of the possible polluters along with the approximate time they passed by the area prior to the spill, along with the distance in the area of *best guess* and area of *uncertainty*.

Table 20. Possible polluters in the SUR2010059_2 Spill Event

IMO	Name	Hours prior to Spill	Distance in Best Guess (nm)	Distance in Uncertainty (nm)
8708244	SOLAR WING	45	0.969	2.842
9059119	SUNNY NAPIER II	55	0.000	3.551
9122887	SEVEN OCEAN	18	0.000	0.045
9162411	GLOBAL CHALLENGER	43	1.247	4.156
9205847	KIND SEAS	67	0.000	3.027
9206140	CRIMSON FOREST	71	0.000	4.864
9310745	ANSAC KATHRYN	42	0.000	3.842
9384863	LASER ACE	3	0.000	1.150

Table 21 shows that the criteria pairwise comparison matrix is the same as the SUR2010059_2 Spill Event, where the time is only moderately more important compared to the distances in *best guess* and *uncertainty* areas. This is because the spill occurred in the open ocean and it is plausible that these spills may have occurred up to 72 hours prior to detection, as opposed to some of the inshore spills where plots were found to have beached prior to the full 72 hour simulation run duration.

Table 21. Criteria Pairwise Comparison Matrix for the SUR2010059_2 Spill Event

	time (hrs)	best guess (Nm)	uncertainty (Nm)
--	------------	-----------------	------------------

time (hrs)	1.00	3.00	4.00
best guess (Nm)	0.33	1.00	2.00
uncertainty (Nm)	0.25	0.50	1.00

From this matrix, the eigenvector is identical to that from the SUR2010059_2 spill event, (0.6250, 0.2385, 0.1365), and the CR is 0.016 which shows consistency in this approach.

For the time a vessel traveled past the area of the spill prior to detection, a scale of 8 hour intervals was applied. Table 22 shows the ranking according to elapsed time for each of the eight vessels

Table 22. Time categorization of the possible polluter in the SUR2010059_2 Spill Event

Vessel Name	Time traveled prior to Spill Detection (hrs)	Category
SOLAR WING	45	6
SUNNY NAPIER II	55	7
SEVEN OCEAN	18	3
GLOBAL CHALLENGER	43	6
KIND SEAS	67	9
CRIMSON FOREST	71	9
ANSAC KATHRYN	42	6
LASER ACE	3	1

From the corresponding matrix built based on Table 22, the eigenvector was found to be (0.0821, 0.0522, 0.2381, 0.0821, 0.0252, 0.0252, 0.0821, 0.4129) with a CR of 0.073.

For the classification of the *Best Guess* and *Uncertainty* areas of the spill, distance scales of 0.5 and 1 nautical miles were used, respectively. Table 23 shows the classification of each alternative.

Table 23. Classification of possible polluters in the SUR2010059_2 Spill Event based on the distance in the area of *best guess* and *uncertainty*

Vessels	Distance in Best Guess (Nautical	Classification for Distance in Best Guess	Distance in Uncertainty (Nautical Miles)	Classification for Distance in Area of Uncertainty
---------	----------------------------------	---	--	--

	Miles)			
SOLAR WING	0.969	2	2.842	3
SUNNY NAPIER II	0.000	1	3.551	4
SEVEN OCEAN	0.000	1	0.045	1
GLOBAL CHALLENGER	1.247	3	4.156	5
KIND SEAS	0.000	1	3.027	4
CRIMSON FOREST	0.000	1	4.864	5
ANSAC KATHRYN	0.000	1	3.842	4
LASER ACE	0.000	1	1.150	2

Following the same technique as for the *time prior to detection* criterion, we end up with eigenvectors (0.1750, 0.0904, 0.0904, 0.2823, 0.0904, 0.0904, 0.0904, 0,0904) and (0.0767, 0.1298, 0.0335, 0.02256, 0.1298, 0.2256, 0.1298, 0.0491) and CR values of 0.002 and 0.022 for the *best guess* and *uncertainty* areas, respectively.

With all the eigenvectors computed, the rankings for each transit were made and the results are shown in Table 24.

Table 24. Ranked possible polluters in the SUR2010059_2 Spill Event

Vessel Name	Normalized Rank
LASER ACE	0.2863
SEVEN OCEAN	0.1750
GLOBAL CHALLENGER	0.1494
SOLAR WING	0.1035
SUNNY NAPIER II	0.0719
ANSAC KATHRYN	0.0906
CRIMSON FOREST	0.0681
KIND SEAS	0.0551

From these results, we see that the 'Laser Ace,' the only vessel headed to Canada, is the

most likely polluter, while the 'Seven Ocean' and 'Global Challenger' finish as the second and third most likely polluters, respectively. Based on this spill along with the SUR2010059_1 spill event, it would appear that both spills came from a polluter headed towards or leaving Canada, since they were close in terms of temporal and physical vicinity. Thus especially as the 'Laser Ace' is only vessel amongst the other 7 vessels headed to Canada and the most likely polluter for event SUR2010059_1, the 'Laser Ace' is our most likely polluter in both of these events.

A fact about the SUR2010059 spill events was that the polluter was actually caught in these events. The spills both came from the same polluter but that vessel (the M/T Champion, a Norwegian flagged vessel) was not detected in LRIT. The vessel was found by radar just prior to entering the Strait of Juan de Fuca, as seen in Figure 30. From LRIT statistics in Canada, about 80% of all SOLAS class vessels (300 GT or higher) are accounted for in this system. The vessel found to be responsible for these spills was an older vessel that was non-compliant to LRIT regulations, thus could not be found in the database for the purposes of this research.



Legend

5025 0 50 Nautical Miles



- ★ SUR2010059 - NASP Detected Spills
- M/T Champion - VTOSS Position Reports

Figure 30. The vessel track of the radar detected M/T Champion, in relationship to the SUR2010059 Spill Events

Chapter 6 Conclusion

In this research, six oil spills, both inshore and offshore on the west coast of Canada were assessed to find the most likely polluter in each of these events. All six of these oil spills were hindcasted to find the possible areas of origin of these spills. In four of the six cases, there was adequate vessel traffic position information, where likely polluters were determined by using the Analytic Hierarchy Process to weight the time and location criteria. However further validation of this ranking has to be done with confirmed polluters found in future oil spills.

In this work, it was found that oil spills can be analyzed on an individual basis. Many countries around the world lack the surveillance efforts for both the monitoring of spills and tracking of vessels to do so. Even though Canada's capability in that regard is very good, there are still information gaps and limitations and not every spill can be analyzed this way, as seen in the SUR2010071 and SUR2010075 cases. There is also a limitation in finding adequate currents data as a lot of the historical data prior to 2010 are either hard to find, or the formatting is too complex for plugging into existing tools. In terms of gaps in vessel traffic data, as the Canadian Coast Guard's AIS network will be fully implemented in the near future, it is believed that much better coverage will be achieved and that many of these gaps in traffic data will be rectified.

Future work includes analyzing historic spills on the east coast of Canada and in the Arctic. Additionally, while the metrics of time and oil spill coverage area were used in the AHP process, further analysis of additional metrics, such as vessel characteristics (ie: vessel type and age) could be considered in this analysis as well. It was also a goal of this research to develop a proof-of concept in hopes of eventually using this technique in real-time. Furthermore, as previously mentioned, this method must be further

scrutinized with a validation process of matching these likely polluters, to the polluters found in known cases to determine its applicability. This research may potentially lead to a change in the way that NASP operates. If a suspected polluter from a previous spill event is traversing a similar area, NASP may actually fly over the areas at the time of transit of that particular vessel to potentially catch the suspected polluter red-handed. Also if vessels are suspected as polluters in multiple cases, this research may provide probable cause to investigate these vessels while at port.

References

- ASCE, "State-of-the-Art Review of Modeling Transport and Fate of Oil Spills", *Journal of Hydraulic Engineering*, 122 (1996): 594-609
- Beegle-Krause, C.J., "General NOAA Oil Modeling Environment (GNOME): A New Spill Trajectory Model", *Proceedings of the 2001 International Oil Spill Conference*, Tampa, FL, March 26-29, 2001. St. Louis, MO: Mira Digital Publishing, Inc. pp. 865-871
- Bradaric, Z., Srdelic, M., Mladineo, N., and Pavasovic, S., "Place of refuge selection for ships aiming at reduction of environmental hazards", *Environmental Problems in Coastal Regions VII*, 99 (2008): 127 – 135
- Canadian Hydrographic Services, "Tides, Currents, and Water Levels" last modified November 2, 2011, -<http://www.charts.gc.ca/publications/ctct-tmcc-eng.asp>
- Cekirge H.M., Koch, M., Long, C., Giammona, C.P., Binkley, K., Engelhardt, R., and Jamail, R., "State-of-the art techniques in oil spill modeling", *Oil Spill Conference, USA, Library of Congress Catalog* (1995): 67-72
- Cheng, Y., Li, X., Xu, G., Garcia-Pineda, O., Andersen, O. B., and Pichel, W.G., "SAR observation and model tracking of an oil spill event in coastal waters", *Marine Pollution Bulletin*, 62 (2011): 350 -363
- Dalton, Tracey, and Jin, Di, "Extent and Frequency of Vessel Oil Spills in US Marine Protected Areas", *Marine Pollution Bulletin*, 60 (2010): 1939-1945
- Divisions of Earth and Life Studies and Transportation Research Board of the National Research Council, "Oil in the Sea III", (2003)
- Environment Canada, "Marine Buoy Observations" Last modified December 30, 2010, - <http://www.ec.gc.ca/meteo-weather/default.asp?lang=En&n=BC223DA3-1>
- Etkin, D.S., "A Worldwide Review of Marine Oil Spills Fines and Penalties," *Environmental Research Consulting* (2003)
- Ferraro, G., Bernardini, A., David, M., Meyer-Roux, S., Muellenhoff, O., Perkovic, M., Tarchi, D., and Topouzelis, K., "Toward an operational use of space imagery for oil pollution monitoring in the Mediterranean basin: A demonstration in the Adriatic Sea," *Marine Pollution Bulletin* 54 (2007): 403-422
- Galt, J.A., "The Integration of Trajectory Models and Analysis into Spill Response Information Systems," *Spill Science and Technology Bulletin* 4 (1997): 123-129
- GESAMP, "Estimates of Oil Entering the Marine Environment from Sea-based Activities," 75 (2007)
- Himes, Amber., "Performance Indicator Importance in MPA Management Using a Multi-Criteria Approach", *Coastal Management*, 35 (2007): 601-618

Hoye, Gudrun K., Eriksen, T., Meland, B.J., and Narheim, B.T., "Space-based AIS for Global Maritime Traffic Monitoring", *Acta Astronautica*, 62 (2008): 240-245

Huang, Ivy., Keisler, J., and Linkov, I., "Multi-criteria decision analysis in environmental sciences: Ten years of applications and trends", *Science of the Total Environment*, 409 (2011): 3578-3594

IFAW, "Slow Death: Deliberate Oil Pollution and Seabirds" IFAW (2008), accessed July 14, 2011, -
http://www.ifaw.org/ifaw_international/join_campaigns/national_regional_efforts/ifaw_in_action_canada/protecting_seabirds/oil_pollution_and_seabirds.php

International Maritime Organization, "Long-range Identification and Tracking of Ships" in SOLAS Safety of Navigation, Chap. 5, 2008

Kim Pearce, National Aerial Surveillance Analyst, personal communication, May 16, 2011.

Norma Serra-Sogas, "Modelling risk of chronic oil pollution from vessel operations in Canada's West Coast" (MSc diss., University of Victoria, 2010).

OEA Technologies, "CODAR HF Radars in Canada" last modified 2011, -
<http://www.oeratech.com/news/a-sense-of-the-sea/codar-hf-radars-in-canada/>

Office of the Auditor General of Canada, Report of the Commissioner of Environment and Sustainable Development to the House of Commons: Chapter 1, Oil Spills from Ships, Report, Ottawa, ON, 2010

Perkovic, Marco., Greidanus, Harm., Muellenhoff, Oliver., Ferraro, Guido., Pavlakis, Petros., Cosoli, Simone., and Harsch, Rick., "Marine Polluter Identification: Backtracking with the aid of Satellite Imaging", *Fresenius Environmental Bulletin*, 19 (2010): 2462 - 2432

Perret, Fabienne., "Marine Traffic Visualization Canada's West Coast" (MSc Diss., University of Victoria, 2003)

Reed, Mark., Johansen, Oistein., Brandvik, Per Johan., Dalin, Per., Lewis, Alun., Fiocco, Robert., Mackay, Don., and Prentki, Richard., "Oil Spill Modeling towards the Close of the 20th Century: Overview of the State of the Art", *Spill Science & Technology Bulletin*, 5 (1999): 3-16

Saaty, Thomas., "The Analytic Hierarchy Process", McGraw-Hill (1990), accessed November 17, 2011

Serra-Sogas, Norma., et al., "Visualization of Spatial Patterns and Temporal Trends for Aerial Surveillance of Illegal Oil Discharges in Western Canadian Marine Waters", *Marine Pollution Bulletin*, 56 (2008): 825-833

Shangan Webservices Inc, "Earls Cove". Last modified January 12, 2012, -

<http://www.vancouverisland.com/regions/towns/?townid=308>

Stankiewicz, Monika and Vlasov, Nikolay, " Helcom achieves a major decrease in illegal oil discharges in the Baltic" HELCOM (2011), accessed July 14, 2011, http://www.helcom.fi/press_office/news_helcom/en_GB/illegal_spills_2010Aerial_surveillance_report/

The Committee on Oil in the Sea "Oil in the Sea III: Inputs, Fates, and Effects" The National Academies Press, 2003

Transport Canada "National Aerial Surveillance Program – July 2010," last modified August 24, 2010, <http://www.tc.gc.ca/eng/mediaroom/backgrounders-b04-m126e-1342.htm>

United Nation Environment Programme, "Global Marine Oil Pollution Information Gateway", last modified January 6, 2005, - <http://oils.gpa.unep.org/about/about.htm>

Wiese, Francis K., Montevecchi, W.A., Davoren, G.K., Huettmann, F., Diamond, A.W., and Linke, J., "Seabirds at Risk around Offshore Oil Platforms in the North-west Atlantic", Marine Pollution Bulletin, 42 (2001): 1285 – 1290

Appendix 1: Wind Data

SUR2010060 Spill Event Winds: Port Hardy Weather Station

Date	Local Time	UTC	Wind Direction	Speed (km/h)	Speed (m/s)	Hours prior to detection
22-Aug	2:00	19:00	23	9	2.50	72
	3:00	20:00	23	7	1.94	71
	4:00	21:00	0	0	0.00	70
	5:00	22:00	0	0	0.00	69
	6:00	23:00	22	6	1.67	68
	7:00	0:00	23	13	3.61	67
	8:00	1:00	24	7	1.94	66
	9:00	2:00	22	9	2.50	65
	10:00	3:00	24	11	3.06	64
	11:00	4:00	2	7	1.94	63
	12:00	5:00	1	7	1.94	62
	13:00	6:00	3	6	1.67	61
	14:00	7:00	1	4	1.11	60
	15:00	8:00	32	9	2.50	59
	16:00	9:00	31	9	2.50	58
	17:00	10:00	32	7	1.94	57
	18:00	11:00	9	9	2.50	56
	19:00	12:00	30	6	1.67	55
	20:00	13:00	0	0	0.00	54
	21:00	14:00	0	0	0.00	53
	22:00	15:00	0	0	0.00	52
	23:00	16:00	0	0	0.00	51
	0:00	17:00	0	0	0.00	50
	1:00	18:00	0	0	0.00	49
	2:00	19:00	0	0	0.00	48

		0				
	3:00	20:0 0	17	4	1.11	47
	4:00	21:0 0	0	0	0.00	46
	5:00	22:0 0	0	0	0.00	45
23- Aug	6:00	23:0 0	0	0	0.00	44
	7:00	0:00	0	0	0.00	43
	8:00	1:00	10	6	1.67	42
	9:00	2:00	10	20	5.56	41
	10:00	3:00	8	20	5.56	40
	11:00	4:00	9	15	4.17	39
	12:00	5:00	11	15	4.17	38
	13:00	6:00	10	9	2.50	37
	14:00	7:00	10	15	4.17	36
	15:00	8:00	16	19	5.28	35
	16:00	9:00	14	6	1.67	34
	17:00	10:0 0	2	7	1.94	33
	18:00	11:0 0	0	0	0.00	32
	19:00	12:0 0	0	0	0.00	31
	20:00	13:0 0	0	0	0.00	30
	21:00	14:0 0	0	0	0.00	29
	22:00	15:0 0	0	0	0.00	28
	23:00	16:0 0	0	0	0.00	27
	0:00	17:0 0	0	0	0.00	26
	1:00	18:0 0	0	0	0.00	25
	2:00	19:0 0	0	0	0.00	24
	3:00	20:0 0	0	0	0.00	23
	4:00	21:0 0	0	0	0.00	22
	5:00	22:0 0	0	0	0.00	21

24- Aug	6:00	23:0 0	0	0	0.00	20
	7:00	0:00	0	0	0.00	19
	8:00	1:00	0	0	0.00	18
	9:00	2:00	11	6	1.67	17
	10:00	3:00	0	0	0.00	16
	11:00	4:00	3	6	1.67	15
	12:00	5:00	9	9	2.50	14
	13:00	6:00	0	0	0.00	13
	14:00	7:00	0	0	0.00	12
	15:00	8:00	0	0	0.00	11
	16:00	9:00	33	6	1.67	10
	17:00	10:0 0	30	6	1.67	9
	18:00	11:0 0	32	7	1.94	8
	19:00	12:0 0	0	0	0.00	7
	20:00	13:0 0	0	0	0.00	6
	21:00	14:0 0	0	0	0.00	5
	22:00	15:0 0	0	0	0.00	4
	23:00	16:0 0	0	0	0.00	3
	0:00	17:0 0	0	0	0.00	2
	1:00	18:0 0	0	0	0.00	1
25- Aug	2:00	19:0 0	0	0	0.00	0

SUR2010044 Spill Event Winds: Tofino Weather Station

Date	UTC	Wind Direction	Speed (km/h)	Speed (m/s)	Hours prior to detection
	21:00	n/a	n/a	n/a	72

21-Jun	22:00	0	0	0.00	71
	23:00	0	0	0.00	70
	0:00	15	4	1.11	69
	1:00	17	6	1.67	68
	2:00	18	9	2.50	67
	3:00	19	11	3.06	66
	4:00	16	9	2.50	65
	5:00	17	15	4.17	64
	6:00	15	11	3.06	63
	7:00	17	11	3.06	62
	8:00	20	9	2.50	61
	9:00	18	9	2.50	60
	10:00	18	11	3.06	59
	11:00	n/a	n/a	n/a	58
	12:00	n/a	n/a	n/a	57
	13:00	n/a	n/a	n/a	56
	14:00	n/a	n/a	n/a	55
	15:00	n/a	n/a	n/a	54
	16:00	n/a	n/a	n/a	53
	17:00	n/a	n/a	n/a	52
	18:00	n/a	n/a	n/a	51
	19:00	n/a	n/a	n/a	50
	20:00	n/a	n/a	n/a	49
21:00	n/a	n/a	n/a	48	
22-Jun	22:00	0	0	0.00	47
	23:00	0	0	0.00	46
	0:00	0	0	0.00	45
	1:00	0	0	0.00	44
	2:00	17	6	1.67	43
	3:00	20	9	2.50	42
	4:00	22	7	1.94	41
	5:00	22	11	3.06	40
	6:00	21	9	2.50	39
	7:00	20	13	3.61	38
	8:00	19	13	3.61	37
	9:00	23	13	3.61	36
	10:00	23	7	1.94	35
	11:00	n/a	n/a	n/a	34
	12:00	n/a	n/a	n/a	33
	13:00	n/a	n/a	n/a	32
14:00	n/a	n/a	n/a	31	

23-Jun	15:00	n/a	n/a	n/a	30
	16:00	n/a	n/a	n/a	29
	17:00	n/a	n/a	n/a	28
	18:00	n/a	n/a	n/a	27
	19:00	n/a	n/a	n/a	26
	20:00	n/a	n/a	n/a	25
	21:00	n/a	n/a	n/a	24
	22:00	31	4	1.11	23
	23:00	0	0	0.00	22
24-Jun	0:00	26	6	1.67	21
	1:00	26	4	1.11	20
	2:00	16	7	1.94	19
	3:00	17	4	1.11	18
	4:00	17	4	1.11	17
	5:00	22	6	1.67	16
	6:00	16	6	1.67	15
	7:00	20	6	1.67	14
	8:00	24	11	3.06	13
	9:00	22	9	2.50	12
	10:00	22	11	3.06	11
	11:00	n/a	n/a	n/a	10
	12:00	n/a	n/a	n/a	9
	13:00	n/a	n/a	n/a	8
	14:00	n/a	n/a	n/a	7
	15:00	n/a	n/a	n/a	6
	16:00	n/a	n/a	n/a	5
	17:00	n/a	n/a	n/a	4
	18:00	n/a	n/a	n/a	3
19:00	n/a	n/a	n/a	2	
20:00	n/a	n/a	n/a	1	
21:00	n/a	n/a	n/a	0	

SUR2010071 Spill Event Winds: Prince Rupert Weather Station

Date	UTC	Wind Direction	Speed (km/h)	Speed (m/s)	Hours prior to detection
28-Oct	22:00	34	13	3.61	72
	23:00	0	0	0.00	71
26-Oct	0:00	0	0	0.00	70
	1:00	0	0	0.00	69
	2:00	10	4	1.11	68
	3:00	31	15	4.17	67
	4:00	31	26	7.22	66
	5:00	31	22	6.11	65
	6:00	31	22	6.11	64
	7:00	32	22	6.11	63
	8:00	30	26	7.22	62
	9:00	31	20	5.56	61
	10:00	30	17	4.72	60
	11:00	30	11	3.06	59
	12:00	28	11	3.06	58
	13:00	28	9	2.50	57
	14:00	26	9	2.50	56
	15:00	25	7	1.94	55
	16:00	21	9	2.50	54
	17:00	19	15	4.17	53
	18:00	13	7	1.94	52
	19:00	11	9	2.50	51
	20:00	13	7	1.94	50
	21:00	11	9	2.50	49
	22:00	10	11	3.06	48
23:00	10	9	2.50	47	
0:00	10	9	2.50	46	
1:00	10	9	2.50	45	
2:00	10	9	2.50	44	
3:00	9	9	2.50	43	
4:00	2	7	1.94	42	
5:00	36	7	1.94	41	
6:00	36	11	3.06	40	
7:00	36	15	4.17	39	
8:00	36	13	3.61	38	
9:00	36	13	3.61	37	
10:00	1	6	1.67	36	
11:00	4	6	1.67	35	

27-Oct	12:00	10	13	3.61	34
	13:00	10	11	3.06	33
	14:00	10	11	3.06	32
	15:00	10	11	3.06	31
	16:00	9	7	1.94	30
	17:00	0	0	0.00	29
	18:00	16	6	1.67	28
	19:00	10	9	2.50	27
	20:00	9	15	4.17	26
	21:00	11	7	1.94	25
	22:00	10	9	2.50	24
28-Oct	23:00	10	11	3.06	23
	0:00	10	9	2.50	22
	1:00	10	6	1.67	21
	2:00	5	6	1.67	20
	3:00	3	6	1.67	19
	4:00	35	11	3.06	18
	5:00	36	6	1.67	17
	6:00	28	6	1.67	16
	7:00	23	6	1.67	15
	8:00	22	6	1.67	14
	9:00	20	6	1.67	13
	10:00	18	7	1.94	12
	11:00	12	7	1.94	11
	12:00	12	6	1.67	10
	13:00	15	7	1.94	9
	14:00	14	9	2.50	8
	15:00	13	9	2.50	7
	16:00	14	11	3.06	6
	17:00	16	13	3.61	5
	18:00	16	13	3.61	4
	19:00	17	20	5.56	3
	20:00	17	17	4.72	2
21:00	16	19	5.28	1	
22:00	17	20	5.56	0	

SUR2010059 Spill Event Winds: Tofino Weather Station

Date	UTC	Wind Direction	Speed (km/h)	Speed (m/s)	Hours prior to detection
26-Jul	20:00	n/a	n/a	n/a	72
	21:00	n/a	n/a	n/a	71
	22:00	15	13	3.61	70
	23:00	14	13	3.61	69
27-Jul	0:00	14	15	4.17	68
	1:00	14	17	4.72	67
	2:00	14	17	4.72	66
	3:00	14	17	4.72	65
	4:00	15	20	5.56	64
	5:00	15	22	6.11	63
	6:00	14	19	5.28	62
	7:00	16	11	3.06	61
	8:00	18	11	3.06	60
	9:00	19	9	2.50	59
	10:00	18	7	1.94	58
	11:00	n/a	n/a	n/a	57
	12:00	n/a	n/a	n/a	56
	13:00	n/a	n/a	n/a	55
	14:00	n/a	n/a	n/a	54
	15:00	n/a	n/a	n/a	53
	16:00	n/a	n/a	n/a	52
	17:00	n/a	n/a	n/a	51
	18:00	n/a	n/a	n/a	50
	19:00	n/a	n/a	n/a	49
	20:00	n/a	n/a	n/a	48
	21:00	n/a	n/a	n/a	47
	22:00	15	11	3.06	46
	23:00	16	7	1.94	45
27-Jul	0:00	15	9	2.50	44
	1:00	16	9	2.50	43
	2:00	16	11	3.06	42
	3:00	17	9	2.50	41
	4:00	16	7	1.94	40
	5:00	20	7	1.94	39
	6:00	19	9	2.50	38
	7:00	21	11	3.06	37
	8:00	20	11	3.06	36
	9:00	21	9	2.50	35

28-Jul	10:00	23	9	2.50	34
	11:00	n/a	n/a	n/a	33
	12:00	n/a	n/a	n/a	32
	13:00	n/a	n/a	n/a	31
	14:00	n/a	n/a	n/a	30
	15:00	n/a	n/a	n/a	29
	16:00	n/a	n/a	n/a	28
	17:00	n/a	n/a	n/a	27
	18:00	n/a	n/a	n/a	26
	19:00	n/a	n/a	n/a	25
	20:00	n/a	n/a	n/a	24
	21:00	n/a	n/a	n/a	23
	22:00	13	13	3.61	22
23:00	14	11	3.06	21	
29-Jul	0:00	14	9	2.50	20
	1:00	15	9	2.50	19
	2:00	15	9	2.50	18
	3:00	16	7	1.94	17
	4:00	21	6	1.67	16
	5:00	20	9	2.50	15
	6:00	22	9	2.50	14
	7:00	30	7	1.94	13
	8:00	30	15	4.17	12
	9:00	27	11	3.06	11
	10:00	25	13	3.61	10
	11:00	n/a	n/a	n/a	9
	12:00	n/a	n/a	n/a	8
	13:00	n/a	n/a	n/a	7
	14:00	n/a	n/a	n/a	6
	15:00	n/a	n/a	n/a	5
	16:00	n/a	n/a	n/a	4
17:00	n/a	n/a	n/a	3	
18:00	n/a	n/a	n/a	2	
19:00	n/a	n/a	n/a	1	
20:00	n/a	n/a	n/a	0	

Appendix 2: The SUR2010044 AHP Analysis – Worked out Example

From Section 5.2, the original criteria pairwise comparison matrix is as follows:

Matrix 1: Original Pairwise Matrix

	Hours Prior to detection	best guess (Nm)	uncertainty (Nm)
Hours Prior to detection	1.00	5.00	6.00
best guess (Nm)	0.20	1.00	3.00
uncertainty (Nm)	0.17	0.33	1.00

*Values rounded to two decimal places

To determine the eigenvector of this matrix, we must perform the following steps:

- 1) Raise the pairwise matrix to powers that are successively squared each time
- 2) Sum the rows and normalize
- 3) When the difference between these sums in two consecutive calculations is consistent up to 4 decimal places, stop the successive squaring of the matrix and obtain the eigenvector

For the original pairwise matrix above (Matrix 1), by squaring it, the following matrix is achieved.

Matrix 2: Squared Criteria Matrix – First Interval

	Hours Prior to detection	best guess (Nm)	uncertainty (Nm)
Hours Prior to detection	3.00	12.00	27.00
best guess (Nm)	0.90	3.00	7.20
uncertainty (Nm)	0.40	1.50	3.00

The sum for each row is (42.00, 11.10 and 4.90) for rows 1 through 3, respectively. The sum of these three rows is 58.00. By normalizing these sums, we are left with the values (0.7241, 0.1914 and 0.0844).

Matrix 2 is then squared.

Matrix 3: Squared Criteria Matrix – Second Interval

	Hours Prior to detection	best guess (Nm)	uncertainty (Nm)
Hours Prior to detection	30.60	112.50	248.40
best guess (Nm)	8.28	30.60	67.50
uncertainty (Nm)	3.75	13.80	30.60

The sum of the three rows is (391.50, 106.38 and 48.15) for rows 1 through 3, respectively. The sum of these three rows is 546.03. By normalizing these sums, we are left with the values (0.7170, 0.1948 and 0.0881).

Matrix 3 is then squared.

Matrix 4: Squared Criteria Matrix – Third Interval

	Hours Prior to detection	best guess (Nm)	uncertainty (Nm)
Hours Prior to detection	2799.36	10312.92	22795.83
best guess (Nm)	759.86	2799.36	6187.75
uncertainty (Nm)	343.76	1266.44	2799.36

The sum of the three rows is (35908.11, 9746.97 and 4409.56) for rows 1 through 3, respectively. The sum of these three rows is 50064.64. By normalizing these sums, we are left with the values (0.7172, 0.1947 and 0.0881).

Matrix 4 is then squared.

Matrix 5: Squared Criteria Matrix – Fourth Interval

	Hours Prior to detection	best guess (Nm)	uncertainty (Nm)
Hours Prior to detection	23509187.82	86608588	1.91E+08
best guess (Nm)	6381375.356	23509188	51965153
uncertainty (Nm)	23509187.82	86608588	1.91E+08

The sum of the three rows is (301559036.94, 81855716.23 and 37031766.36) for rows 1 through 3, respectively. The sum of these three rows is 420446519.53. By normalizing these sums, the values of the normalized row sums provide the 3 x 1 matrix, (0.7172, 0.1947 and 0.0881).

This is consistent with the value found after the third interval of squaring, thus the process stops here as the result is the eigenvector for Matrix 1.

From equation 4, the next step is to find $\sum_{j=1}^n a_{ij} w_j$. From Matrix 1, for row 1, this is done by a series of calculation is as follows:

$$\sum_{j=1}^n a_{1,j} w_j = 1.00 * 0.7172 + 5.00 * 0.1947 + 6.00 * 0.0881 = 2.2191$$

For row 2:

$$\sum_{j=1}^3 a_{2,j} w_j = 0.20 * 0.7172 + 1.00 * 0.1947 + 3.00 * 0.0881 = 0.6024$$

For row 3:

$$\sum_{j=1}^3 a_{3,j} w_j = 0.17 * 0.7172 + 0.33 * 0.1947 + 1.00 * 0.0881 = 0.2725$$

The next step is to determine λ_{max} by dividing the above values by their respective eigenvalues:

$$\lambda_{max} = \frac{\sum_{j=1}^n a_{i,j} w_j}{w_i} = \frac{2.2191}{0.7172} = \frac{0.6024}{0.1947} = \frac{0.2725}{0.0881} = 3.0940$$

With λ_{max} computed, the consistency index is calculated according to equation 6:

$$CI = \frac{\lambda_{max} - n}{n - 1} = \frac{3.0940 - 3}{3 - 1} = 0.0470$$

The next step is to determine the consistency ratio according to equation 7:

$$CR = CI/RI = 0.0470/0.58 = 0.0810$$

This value of the consistency ratio provides a value less than 10%, which ensures consistency, thus this eigenvector is valid for application.

The above process is repeated for each of the 4 vessels under each criteria. The following values were obtained for each:

Matrix 6: The original pairwise comparison matrix of vessels in the SUR2010044 spill for the time traveled prior to spill detection criteria

FRANCES BARKLEY (1)	FRANCES BARKLEY (2)	JACK BRUSCO	PACIFIC CREST
------------------------	------------------------	----------------	------------------

FRANCES BARKLEY (1)	1.00	0.50	3.00	2.00
FRANCES BARKLEY (2)	2.00	1.00	4.00	3.00
JACK BRUSCO	0.33	0.25	1.00	0.50
PACIFIC CREST	0.50	0.33	2.00	1.00

Where the eigenvector was determined as (0.2772, 0.4673, 0.954, 0.1601) with a CR of 0.018.

Matrix 7: The original pairwise comparison matrix of vessels in the SUR2010044 spill for the distance traveled in the area of *best guess*

	FRANCES BARKLEY (1)	FRANCES BARKLEY (2)	JACK BRUSCO	PACIFIC CREST
FRANCES BARKLEY (1)	1.00	2.00	4.00	0.50
FRANCES BARKLEY (2)	0.50	1.00	3.00	0.33
JACK BRUSCO	0.25	0.33	1.00	0.20
PACIFIC CREST	2.00	3.00	5.00	1.00

Where the eigenvector was determined as (0.2844, 0.1699, 0.0729, 0.4729) with a CR of 0.029.

Matrix 8: The original pairwise comparison matrix of vessels in the SUR2010044 spill for the distance traveled in the area of *uncertainty*

	FRANCES BARKLEY (1)	FRANCES BARKLEY (2)	JACK BRUSCO	PACIFIC CREST
FRANCES BARKLEY (1)	1.00	1.00	0.20	0.17
FRANCES BARKLEY (2)	1.00	1.00	0.20	0.17
JACK BRUSCO	5.00	5.00	1.00	0.50
PACIFIC CREST	6.00	6.00	2.00	1.00

Where the eigenvector was determined as (0.0751, 0.0751, 0.3329, 0.5168) with a CR value of 0.019.

Lastly by multiplying the 4x3 eigenvector matrix against the 3x1 criteria eigenvector, the rankings are determined:

	time (hrs)	best guess	uncertainty		
FRANCES BARKLEY (1)	0.2772	0.2844	0.0751	x	0.7172
FRANCES BARKLEY (2)	0.4673	0.1699	0.0751		0.1947
JACK BRUSCO	0.0954	0.0729	0.3329		0.0881
PACIFIC CREST	0.1601	0.4729	0.5168		

Thus the final result is achieved:

Vessels	Normalized Results
FRANCES BARKLEY (1)	0.2608
FRANCES BARKLEY (2)	0.3749
JACK BRUSCO	0.1120
PACIFIC CREST	0.2524